



**HAL**  
open science

# Volumetric properties of furan and 2-5-dimethylfuran in different industrial solvents at temperatures from 278 to 343 K

Mohsin Ali Raza, Alain Valtz, Christophe Coquelet, Paul D Hallett, Waheed Afzal

## ► To cite this version:

Mohsin Ali Raza, Alain Valtz, Christophe Coquelet, Paul D Hallett, Waheed Afzal. Volumetric properties of furan and 2-5-dimethylfuran in different industrial solvents at temperatures from 278 to 343 K. *Journal of Chemical and Engineering Data*, 2021, 66 (7), pp.2666-2680. 10.1021/acs.jced.0c01060 . hal-03281344

**HAL Id: hal-03281344**

**<https://hal.science/hal-03281344>**

Submitted on 8 Jul 2021

**HAL** is a multi-disciplinary open access archive for the deposit and dissemination of scientific research documents, whether they are published or not. The documents may come from teaching and research institutions in France or abroad, or from public or private research centers.

L'archive ouverte pluridisciplinaire **HAL**, est destinée au dépôt et à la diffusion de documents scientifiques de niveau recherche, publiés ou non, émanant des établissements d'enseignement et de recherche français ou étrangers, des laboratoires publics ou privés.

Volumetric properties of furan and 2-5-dimethylfuran in different industrial solvents at temperatures from 278 to 343 K

Mohsin Ali Raza<sup>1,2</sup>, Alain Valtz<sup>2</sup>, Christophe Coquelet<sup>2\*</sup>, Paul D. Hallett<sup>3</sup>,  
Waheed Afzal<sup>1\*</sup>

<sup>1</sup>School of Engineering, University of Aberdeen, Aberdeen AB24 3UE,  
Scotland, United Kingdom.

<sup>2</sup>MINES ParisTech PSL University, CTP-Centre of Thermodynamics of  
Processes, 35 Rue Saint Honoré, 77305 Fontainebleau, France.

<sup>3</sup>School of Biological Sciences, University of Aberdeen, Aberdeen AB24 3UU,  
Scotland, United Kingdom.

\*Corresponding author at MINES ParisTech PSL University: Christophe  
Coquelet (christophe.coquelet@mines-paristech.fr)

\*Corresponding author at University of Aberdeen: Waheed Afzal  
(waheed@abdn.ac.uk)

## Abstract

Density and Speed of sound have been measured for pure components such furan, (DMF) 2-5-dimethylfuran, MDEA (n-methyldiethanolamine), DEG (diethylene glycol), TEG (triethylene glycol), and DMA (dimethylacetamide) using Anton Paar (DSA-5000) vibrating U-tube densitometer in a temperature range of 278.15 to 343.15 K and ambient pressure (100 kPa). density and speed of sound have been measured for furan + MDEA, furan + DEG, furan + TEG, and furan + DMA in a temperature range of 278.15 K to 303.15 K whereas for DMF + DMA, the temperature range is 283.15 K to 343.15 K. excess molar volume have been calculated for all binary systems. The Redlich–Kister model is used to correlate the experimental data. In order to identify the impact of molecular interactions participating significantly in the excess molar volume, the Prigogine–Flory–Patterson model is selected to correlate and predict the deviations for excess molar volumes of the binary mixtures.

**Keywords:** Density, excess molar volume, furan, 2-5-dimethylfuran, RK model, PFP model

## **Introduction**

Molar excess volume is the property of mixture which is important in both optimizations of current industrial and designing the new processes. Designing several industrial plant units such as heat exchangers, distillation columns, liquid-liquid extractors, and storage tanks require good estimation of density, excess volume, and speed of sound for different mixtures. This manuscript is part of our campaign to providing high-quality experimental data of volumetric properties of industrial fluids and their mixtures<sup>1</sup> Second-generation biofuel or mixtures of such oxygenated compounds known as furan and 2-5-dimethylfuran involve different molecules for which thermodynamic data is unknown. Mixing of these biofuels and oxygenated compounds with industrial solvents such as *n*-methyldiethanolamine (MDEA), diethylene glycol (DEG) triethylene glycol (TEG), and diethanolamine (DEA) behave non-ideally, and deviations from ideal behavior can be expressed in terms of excess properties conveniently.

Excess properties are also useful to explain the intermolecular interactions between mixture molecules. Molecular interaction information provides influential support in selecting the solvent for designing purposes. Solvents are selected based on extracting the desired molecules and removal of undesired molecules from a mixture. Literature shows that the Prigogine–Flory–Patterson model is a handy tool to investigate the excess properties of liquid mixtures.<sup>2-4</sup>

For excess volume, new experimental measurements of density and excess volume for the binary mixtures; furan + *n*-methyldiethanolamine, furan + diethylene glycol, furan + triethylene glycol, furan + dimethylacetamide, and 2-5-dimethylfuran + dimethylacetamide at different temperature ranges are presented. Then, this new experimental data for excess volume is correlated by the Redlich–Kister correlation, and then the Prigogine–Flory–Patterson (PFP) model is applied to determine the predominant intermolecular interactions.<sup>5-7</sup>

## **Materials and methods**

### **Materials**

Table 1 shows the chemical species, supplier, and purity of chemicals used in this work to measure the density, and speed of sound of pure and binary mixtures.

### **Speed of sound and density measurements**

Densities of binary mixtures and pure compounds were measured using an Anton Paar (model DSA-5000) vibrating U-tube densitometer (VTD), in which temperature was controlled by assigning set points in densitometer software with an uncertainty of  $u(T) = 0.01$  K. The densitometer is not equipped with pressure transducer. In consequence, the value of atmospheric pressure is given by GE Druck DPI 142, Precision Barometric Indicator with an accuracy of  $u(P) = 0.035$  kPa. All the mixtures were prepared gravimetrically using Melter balance (model XS205) with an uncertainty of  $u(m) = 0.1$  mg. The oscillating frequency, measured by a densitometer, is dependent on the tube mass containing fluid in it. Uncertainty of the measured experimental data is estimated to be lower than the  $5 \times 10^{-5}$  g.cm<sup>-3</sup>. This density meter can measure the speed of sound with an uncertainty of 0.5 m. sec<sup>-1</sup>. After the measurement of each sample, the apparatus was cleaned with distilled water and anhydrous ethanol. The vibrating element was dried by running the ambient air. isotherm density of the lab air was then measured to verify that the calibration is still valid. If the calibration is not valid, the vendor is called to re-calibrate the apparatus (typically, after several years of use).

To prepare the binary mixtures empty glass vials of 10 cm<sup>3</sup> were closed with a septum and then put under vacuum by introducing a syringe needle connected with a vacuum pump. After vacuum, the empty bottle was weighed, and then solvent or heavier component as component 2 was added using a syringe and put under vacuum again to degas the heavy component and weighed. Then component 1, such as furan or 2-5-dimethylfuran was added and weighed again to calculate the molar fraction of furan in a heavier component. Maximum uncertainty resulting in excess volume calculations were estimated to be less than  $u(v^E) = 0.07$  cm<sup>3</sup>.mol<sup>-1</sup> using Eqs (1 – 3).

$$u_{\rho m} = \sqrt{u_{\rho}^2 + u_x^2} \quad (1)$$

$$u_{x1} = x_1 x_2 u_m \sqrt{\frac{1}{m_1^2} + \frac{1}{m_2^2}} \quad (2)$$

$$u_{v^E} = \sqrt{\left(\left(\frac{x_1 M_1 + x_2 M_2}{\rho_m^2}\right)^2 + \left(\frac{x_1 M_1}{\rho_1^2}\right)^2 + \left(\frac{x_2 M_2}{\rho_2^2}\right)^2\right) u_{\rho m}^2 + \left(\frac{M_1 + M_2}{\rho_m} - \frac{M_1}{\rho_1} + \frac{M_2}{\rho_2}\right)^2 u_x^2} \quad (3)$$

where  $x_i$  is the mole fraction of component  $i$ ,  $M_i$  is the molar mass of component  $i$ ,  $\rho_m$  is the density of the mixture, and  $\rho_i$  is the density of component  $i$ .

Before and after every measurement VTD was rinsed with double distilled water followed by ethanol and dried with an air pump built-in the density meter.

## Results and discussion

## Density and excess volume

The density values of pure compounds measured in this work are compared with the literature data and presented in Table 2; the general agreement between the data set measured from this work and those from the literature is good. The density and speed of sound data for pure furan were measured and compared with the literature (Coquelet et al.<sup>8</sup>). These density values were used to determine the pure component properties and parameters for the Redlich Kister and the PFP models. The density values and speed of sound for nine binary compositions of each system with an increment of 0.1 mole fraction were measured. These density and speed of sound values were used to calculate the excess volume using Eq. (4).

$$v^E = v - x_1v_1^* - x_2v_2^* \quad (4)$$

Where  $x_i$  is a mole fraction and  $v_i^*$  is the molar volume of component  $i$ .  $v$  is the molar volume of mixture and  $v^E$  is the molar excess volume.

Eq. (4) can be rewritten in terms of density to calculate the molar excess volume for a binary mixture using experimental density values.

$$v^E = \left( \frac{x_1M_1 + x_2M_2}{\rho} \right) - \frac{x_1M_1}{\rho_1^*} - \frac{x_2M_2}{\rho_2^*} \quad (5)$$

where  $x_i$  is a mole fraction and  $\rho_i^*$  is the density of component  $i$ .  $M_i$  is the molar mass of component  $i$  and  $v^E$  is the molar excess volume.

## Redlich–Kister Data Treatment

Redlich–Kister<sup>9</sup> (RK) correlation in Eq. (6) was used to correlate the molar excess volume of binary systems.

$$v^E = x_1x_2\sum_i a_i(x_1 - x_2)^i \quad (6)$$

The variance ( $\sigma$ ), corresponding to each fit was determined using Eq. (7)

$$\sigma = \sqrt{\sum \frac{(v^E - v_{cal}^E)^2}{N_{exp} - P}} \quad (7)$$

where  $N_{exp}$  donates the number of experimental data and  $P$  is the number of parameters ( $a_i$ )

The major problem of the RK method is the selection of  $a_i$  the number of parameters. In order to resolve that, it is recommended to compare  $v^E/x_1x_2$  as a function of the molar composition of furan as a lighter compound  $x_1$ , which gives us useful information regarding volumetric properties at low concentrations (Desnoyer and Perron<sup>10</sup>).  $v^E/x_1x_2$  is directly dependent on the apparent molar volume as shown in Eq. (5).

Desnoyers and Perron reported that change in slope is dependent on various factors such as the size of molecules, shape of molecules, intermolecular interaction energy differences at infinite dilution, and formation of the complex having, unlike molecules. At infinite dilutions  $v^E/x_1x_2$ , decreases corresponding to the apparent molar volume which is dependent on the volume of the molecule and free volume space. The number of the RK parameters for all binary systems studied in this work are selected based on analysis of the evolution of  $v^E/x_1x_2$  value as a function of  $x_1$ . The partial molar volume of each component is calculated using the Eq. (8)

$$v_i = v^E + v_i^* + (1 - x_i) \left( \frac{\partial v^E}{\partial x_i} \right)_{P,T} \quad (8)$$

where  $v_i$  is the partial molar volume of component  $i$ ,  $v_i^*$  is the molar volume of pure component  $i$ .  $\frac{\partial v^E}{\partial x_i}$  the term was obtained by differentiating Eq 6, which leads to Eq 9 and Eq 10 for calculating the partial molar volume of components 1 as solute and 2 as solvent of binary mixture respectively.

$$v_1 = v_1^* + (1 - x_1)^2 [\Sigma_o^n a_n (2x_1 - 1)^{n-1} (2(n + 1)x_1 - 1)] \quad (9)$$

$$v_2 = v_2^* + (x_1)^2 [\Sigma_o^n a_n (2x_1 - 1)^{n-1} (2(n + 1)x_1 - (2n + 1))] \quad (10)$$

Table 3 shows the experimental results for density and molar excess volume of MDEA and furan binary mixture at nine different molar fractions and pure components whereas Table 4 shows RK parameters at a temperature range between 278.15 K and 303.15 K with an increment of 5 K. Desnoyers and Perron's method is used for selection of five RK parameters. Figures 1 and 2 present  $v^E$  and  $v^E/x_1x_2$  as a function of  $x_1$ , at temperature 278.15 K and 303.15 K. There's no particular behavior observed; therefore, we can consider that its mixture of two components of similar size. As we can see that, molar volumes are in the negative range as a function  $x_1$ , this is possibly due to dipole-dipole interactions.

Tables 5 and 6 show the excess volume and experimental density values for furan in DEG and TEG respectively at six different temperatures covering the boiling point range of furan. Several molar fractions studied for the different binary mixture are fixed in this study. Tables 7 and 8 show RK parameters determined using experimental data at different temperatures. Figures 3, 4 and Figures 5, 6 present  $v^E$  and  $v^E/x_1x_2$  as a function of  $x_1$ , and show that molar excess volumes are in negative range and maximum value in the negative range has been observed for TEG which is due to an increase in molar mass as compare to DEG and offers

stronger intermolecular interactions resulting, more decrease in excess volume in comparison to DEG.

Tables 9 and 10 show the values of calculated excess volume from the experimental density at different temperature ranges for furan + DMA and DMF + DMA respectively. The temperature range used for DMA and furan was 278.15 K to 303.15 K with a step increment of 5K whereas for DMA with 2-5-dimethylfuran was 283.15 K to 343.15 K with a step increment of 10 K. Therefore, total studied temperatures for DMA in furan are six and for DMA in 2-5-dimethylfuran are seven. Tables 11 and 12 show RK parameters and variance determined using experimental data at different temperatures. Figures 7, 8, and Figure 9, 10 present  $v^E$  and  $v^E/x_1x_2$  as a function of  $x_1$ , for furan + DMA and DMF + DMA respectively, both binary systems show negative values of excess volume, indicating packing effect or attractive interactions occurred. By comparing two binary mixture excess volumes at 298.15 K, it can be observed that DMA with furan shows more negative values as compare to DMA with DMF which concludes that molecular interactions between DMA and furan are stronger.

Figures 11, 12, 13, 14, and 15 show the trend of partial molar volumes of the binary systems studied in this work at two different temperatures such as initial and final temperature. Using RK parameters determined by fitting the RK model to experimental data for each binary system, we plotted the partial molar volumes of furan in MDEA, DEG, TEG, DMA, and DMF in DMA. For MDEA, DEG, TEG, and DMA in furan two temperatures 278.15 K and 303 K data is plotted whereas for DMA in DMF presented temperatures are 283.15 K and 343.15 K. The apparent molar volume is a significant property to define the intermolecular interactions between solute and solvent molecules. At infinite dilutions these partial molar volumes and apparent molar volumes are identical. Deviation of partial molar volume from the apparent molar volume is seemingly more important for infinite dilutions. Figure 13 shows a significant deviation occurs in a region with higher molar fractions of TEG. These deviations are more important at higher values of temperature, in comparison with the other systems studied in this work. There are two possibilities to explain these deviations, one is by increasing the number of RK parameters to correlate with experimental data but it is difficult to do that considering the uncertainty and fact that  $v^E/x_1x_2$  as a function  $x_1$  are well correlated, and another possibility is because of intermolecular interactions between furan and TEG are different than the other systems studied in this work. Therefore, another model should be used for data treatment to identify this kind of molecular interactions and deviations.

### **P-F-P model**



The Prigogine–Flory–Patterson model (PFP) was proposed to study excess thermodynamic properties of polar mixtures<sup>11–15</sup>. Using the same idea some scientists used the Flory model to predict the excess volume whereas others used Prigogine–Flory–Patterson theory<sup>16–20</sup>. The equation of state used in the PFP model was derived for pure compounds and mixture as shown in Eq. (11).

$$\frac{\left(\frac{P}{P^*}\right)\left(\frac{v}{v^*}\right)}{\frac{T}{T^*}} = \frac{\left(\frac{v}{v^*}\right)^{\frac{1}{3}}}{\left(\frac{v}{v^*}\right)^{\frac{1}{3}} - 1} - \frac{1}{\left(\frac{v}{v^*}\right)\left(\frac{T}{T^*}\right)} \quad (11)$$

Where  $T^*$ ,  $P^*$ , and  $v^*$ , are the parameters obtained from thermodynamic data of pure components.

Excess volume calculations are based on the PFP model which describes the interaction between two or more chemical species. Physical interaction which explains the thermodynamic behavior of mixtures is dependent on three parameters such as interactional contribution, free volume contribution, and  $P^*$  contribution. The interactional contribution is proportional to the Flory parameter ( $X_{12}$ ) also known as the cross parameter and it defines the energy changes that happen during the formation of contacts between different molecules. Flory parameter can be determined using the Hildebrand solubility parameter  $\delta_1$  shown in Eq 12<sup>8</sup>.

$$X_{12} = \frac{v(\delta_1 - \delta_2)^2}{RT} + \beta \quad (12)$$

where  $\beta$  is an empirical constant with a value of 0.34 and  $v$  is the molar volume of pure liquid. The solubility parameter  $\delta$  is defined by  $\delta = \sqrt{\frac{\Delta h_v - RT}{v}}$ , with  $\Delta h_v$  the enthalpy of vaporization of the chemical specie. In this form, it is not applicable for polar compound. However, Hansen proposed to modify its expression and proposed that the solubility parameter is the contribution of dispersion forces, intermolecular forces, and hydrogen bonds<sup>21</sup>.

The  $X_{12}$  parameter can be modified using experimental data. Initially, this model was derived for the solubility investigation of polymers in a solvent. Free volume contribution explains the difference in the degree of thermal expansion between mixture molecules.  $P^*$  contribution explains the difference in internal pressure and reduced volume of pure components.

Experimental data of density and speed of sound are used to define the mathematical expression shown in Eq. (14) for the different thermodynamic properties of pure components

such as thermal expansion coefficient ( $\alpha_i$ ), isothermal compressibility factor  $K_{Ti}$  which is related to the isentropic compressibility  $K_s$  via Maxwell's relation in Eq 13

$$K_{Ti} = K_s + \alpha^2 v_i^o \left( \frac{T}{c_p} \right) \quad (13)$$

where  $v_i$  is the molar volume of component  $i$ ,  $K_s$  is the isentropic compressibility  $K_s = -\left(\frac{1}{v}\right) \left(\frac{\partial v}{\partial p}\right)_s$  and can be calculated from the speed of sound and density. speed of sound,

density, and isentropic compressibility in the liquid phase are linked by relation  $c = \sqrt{\left(\frac{1}{K_s \rho}\right)}$ .

Table 13 shows the speed of sound of pure components for MDEA, DEG, TEG, DMA, and DMF. Values of liquid heat capacities  $C_p$  ( $\text{J. mol}^{-1} \cdot \text{K}^{-1}$ ) are taken from the literature<sup>22-25</sup>.

$$f(T) = aT^2 + bT + c \quad (14)$$

Tables 14 – 18 show the values of the a, b, and c parameters for different pure components, with a standard uncertainty of each fitted parameter.

Tables 19 – 24 show values of  $\alpha$ ,  $K_T$ ,  $K_s, v_i^*$ , and  $v_i^o$  used in the PFP model at different temperatures whereas Table 25 shows these values at higher temperatures for DMF + DMA. PFP model was applied to correlate the excess volume of binary systems at six different temperatures to optimize the Flory parameter ( $X_{12}$ ). In order to adjust the Flory parameter, we have used Eq. (15) to minimize the difference between experimental and PFP excess volume values using PFP parameters calculated using Eq. (14) for pure components.

$$D = \sum_i (v_{e,i}^E - v_{PFP,i}^E)^2 \quad (15)$$

The values of the Flory parameter for each binary system at different temperatures are presented in Table 26 and Table 27 whereas Table 28 shows data for DMF + DMA at temperatures 313.15, 323.15, 333.15, and 343.15 K. Flory parameter ( $X_{12}$ ) was initially independent of the composition of the binary mixture<sup>21</sup>, but was used to present the volumetric properties of the polymer and solvent mixtures where  $X_{12}$  depends on the properties of the solvent such as molar volume. Therefore, we consider both species as a solvent, especially when the molar fraction is close to 0.5. Mulder and Smolders mentioned in their work that excess properties are strongly dependent on concentration and indicated that  $X_{12}$  can be determined from excess Gibbs energy<sup>26</sup>. Coquelet et al.<sup>8</sup> in their work also applied an  $X_{12}$  dependent on volume fraction ( $\Phi_1$  and  $\Phi_2$ ). In effect, Hansen reported that

solubility parameter which accounts for dispersive, polar, and hydrogen bonding, which are dependent on concentration<sup>21</sup>. Hence, we modified the  $X_{12}$  by using Eq 16

$$X_{12} = X_{12}^0(a + b(\phi_1 - \phi_2)) \quad (16)$$

Here  $X_{12}^0$  was calculated with no composition dependency of the binary mixture and then  $a, b$  parameters were adjusted using Eq. (15) and considering  $X_{12}^0$  as constant.

Figures 16 – 20 show the difference between the two treatments and concludes that the Flory parameter ( $X_{12}$ ) is composition dependent. As we can observe that the PFP model shows a better correlation when  $X_{12}$  is composition dependent. Tables 29 – 33 present the different contributions to the PFP model for all the five binary systems at different temperatures. PFP model highlights that  $X_{12}$  is compositions dependent for all systems and reflects the presence of H-bonding and polar interactions which are linked with the composition to define the Flory parameter  $X_{12}$ . Figure 21 shows the temperature dependency of the  $X_{12}$  parameter.

The PFP model explain the major contributors for the binary mixtures such as for MDEA + furan are free volume, DEG + furan are free volumes and interactional effect, TEG + furan are free volume and pressure effect, DMA + furan is interactional, and DMA + DMF are pressure effect and interactional effect. Results show that an increase in solvent molecular size affects the interactional effect by dominating the pressure effect in DEG + furan and TEG + furan. Whereas, solute molecule size increase causes a significant increase in the pressure effect and interactional effect as compare to free volume.

The temperature effect shows that DMA + DMF reflects constant interactional forces with temperature increase whereas all other binary systems show an increase in interactional forces, with temperature increase.

## Conclusion

The densities of five binary mixtures (MDEA + furan, DEG + furan, TEG + furan, DMA + furan, and DMA + DMF) are measured over a temperature range between 278 K and 303 K except for DMA + DMF for which temperature range is between 283 K and 343 K. Density and speed of sound for each pure component is measured and used to calculate the molar excess volumes. Redlich-Kister model is used to correlate the experimental data concluding that the RK model correlates well with all five systems except TEG + furan binary systems which shows deviations at infinite dilutions of furan. All systems showed negative values of excess volumes. Prigogine–Flory–Patterson (PFP) model is tested to predict the molar excess

volume of binary mixtures and concluded that it highlights the composition dependence to correlate the experimental data. A provisional treatment of a composition dependence is performed, and results are well represented. PFP model concluded that interactional forces are strongly temperature-dependent as compare to free volume and pressure effect and molecular size shows a significant decrease in the excess volume. The composition effect is also attributed by the PFP model and properly correlates the experimental findings for all binary systems with minimum uncertainties in the calculations.

## References

- 1) Afzal, W., Mohammadi, A.H. and Richon, D., 2009. Volumetric properties of mono-, di-, tri-, and polyethylene glycol aqueous solutions from (273.15 to 363.15) K: experimental measurements and correlations. *J. Chem. Eng. Data*, 54, pp.1254-1261.
- 2) Flory, P.D., 1965. Statistical thermodynamics of liquid mixtures. *J. Am. Chem. Soc.* 87, pp.1833-1838.
- 3) Abe, A. and Flory, P.J., 1965. The thermodynamic properties of mixtures of small, nonpolar molecules. *J. Am. Chem. Soc.*, 87, pp.1838-1846.
- 4) Costas, M. and Patterson, D., 1982. Volumes of mixing and the P\* effect: Part II. Mixtures of alkanes with liquids of different internal pressures. *J. Solution Chem.*, 11, pp.807-821.
- 5) Tôrres, R.B. and Francesconi, A.Z., 2003. Modeling of excess molar volume of binary mixtures of acetonitrile with amines using the prigogine-flory-patterson theory. *J. Mol. Liq.*, 103, pp.99-110.
- 6) Kermanpour, F. and Kheyraadi, Z.G., 2020. Experimental Study of Some Thermodynamic Properties of Binary Mixtures Containing 3-Amino-1-propanol, 2-Aminoethanol, and 1-Butanol at Temperatures of 293.15–333.15 K to Model the Excess Molar Volumes Using the PFP Theory. *J. Chem. Eng. Data*, 65, pp.5360-5368.
- 7) Iloukhani, H. and Almasi, M., 2011. Densities and excess molar volumes of binary and ternary mixtures containing acetonitrile+ acetophenone+ 1, 2-pentanediol: Experimental data, correlation and prediction by PFP theory and ERAS model. *J. Solution Chem.*, 40, pp.284-298.
- 8) Coquelet, C., Auger, E. and Valtz, A., 2019. Density and excess volume for four systems involving eugenol and furan. *J. Solution Chem.*, 48, pp.455-488.
- 9) Redlich, O. and Kister, A.T., 1948. Algebraic representation of thermodynamic properties and the classification of solutions. *Ind. Eng. Chem.*, 40, pp.345-348.
- 10) Desnoyers, J.E. and Perron, G., 1997. Treatment of excess thermodynamic quantities for liquid mixtures. *J. Solution Chem.*, 26, pp.749-755.
- 11) Patterson, D. and Delmas, G., 1970. Corresponding states theories and liquid models. *Discuss. Faraday Soc.*, 49, pp.98-105.

- 12) Gepert, M., Zorębski, E. and Leszczyńska, A., 2005. Is Flory's model the best tool for studying the thermodynamic properties of any kind of binary mixtures?: A critical study of selected binary systems of hydrocarbons. *Fluid Phase Equilib.*, 233, pp.157-169.
- 13) Galvao, A.C. and Francesconi, A.Z., 2008. Application of the Prigogine–Flory–Patterson model to excess molar enthalpy of binary liquid mixtures containing acetonitrile and 1-alkanol. *J. Mol. Liq.*, 139, pp.110-116.
- 14) Tôrres, R.B., Francesconi, A.Z. and Volpe, P.L.O., 2004. Thermodynamics of binary liquid mixtures: application of the Prigogine–Flory–Patterson theory to excess molar volumes of acetonitrile+ 1-alkanol systems. *J. Mol. Liq.*, 110, pp.81-85.
- 15) Rani, M. and Maken, S., 2013. Excess molar enthalpies and excess molar volumes of formamide+ 1-propanol or 2-propanol and thermodynamic modeling by Prigogine–Flory–Patterson theory and Treszczanowicz–Benson association model. *Thermochim. Acta*, 559, pp.98-106.
- 16) Piñeiro, Á., Amigo, A., Bravo, R. and Brocos, P., 2000. Re-examination and symmetrization of the adjustable parameters of the ERAS model: Review on its formulation and application. *Fluid Phase Equilib.*, 173, pp.211-239.
- 17) Flory, P.D., 1965. Statistical thermodynamics of liquid mixtures. *J. Am. Chem. Soc.*, 87, pp.1833-1838.
- 18) Iloukhani, H. and Rezaei-Sameti, M., 2006. Volumetric properties of methylcyclohexane with n-alkanes (C5–C10) at 293.15, 298.15 and 303.15 K—comparison with Prigogine–Flory–Patterson theory. *J. Mol. Liq.*, 126, pp.62-68.
- 19) Valtz, A., Coquelet, C., Boukais-Belaribi, G., Dahmani, A. and Belaribi, F.B., 2011. Volumetric properties of binary mixtures of 1, 2-dichloroethane with polyethers from (283.15 to 333.15) K and at atmospheric pressure. *J. Chem. Eng. Data*, 56, pp.1629-1657.
- 20) Benabida, H., Coquelet, C. and Belaribi, F.B., 2019. Densities and Excess Molar Volumes of the Ternary System (1, 4-Dioxane+ 2-Propanol+ 1, 1, 2, 2-Tetrachloroethane) at T= 288.15–318.15 K and at Atmospheric Pressure: Experimental Measurements and Prigogine–Flory–Patterson Modeling. *J. Chem. Eng. Data*, 64, pp.5122-5131.
- 21) Hansen, C.M., 2002. *Hansen solubility parameters: a user's handbook*. CRC press.
- 22) Li, C.K., Soriano, A.N. and Li, M.H., 2009. Heat capacities of the mixed-solvents desiccants (glycols+ water+ salts). *Thermochim. Acta*, 487, pp.26-32.

- 23) Chiu, L.F., Liu, H.F. and Li, M.H., 1999. Heat capacity of alkanolamines by differential scanning calorimetry. *J. Chem. Eng. Data*, 44, pp.631-636.
- 24) Smirnova, N.N., Tsvetkova, L.Y., Bykova, T.A. and Marcus, Y., 2007. Thermodynamic properties of N, N-dimethylformamide and N, N-dimethylacetamide. *J. Chem. Thermodyn.*, 39, pp.1508-1513.
- 25) Jeżak, S., Dzida, M. and Zorębski, M., 2016. High pressure physicochemical properties of 2-methylfuran and 2, 5-dimethylfuran—second generation biofuels. *Fuel*, 184, pp.334-343.
- 26) Mulder, M.H.V. and Smolders, C.A., 1984. On the mechanism of separation of ethanol/water mixtures by pervaporation I. Calculations of concentration profiles. *J. Membr. Sci.*, 17, pp.289-307.
- 27) Chirico, R.D., Frenkel, M., Magee, J.W., Diky, V., Muzny, C.D., Kazakov, A.F., Kroenlein, K., Abdulagatov, I., Hardin, G.R., Acree Jr, W.E. and Brenneke, J.F., 2013. Improvement of quality in publication of experimental thermophysical property data: Challenges, assessment tools, global implementation, and online support. *Journal of Chemical & Engineering Data*, 58, pp.2699-2716.
- 28) Manuel Bernal-García, J., Guzmán-López, A., Cabrales-Torres, A., Rico-Ramírez, V. and Iglesias-Silva, G.A., 2008. Supplementary densities and viscosities of aqueous solutions of diethylene glycol from (283.15 to 353.15) K. *Journal of Chemical & Engineering Data*, 53, pp.1028-1031.
- 29) Sagdeev, D.I., Fomina, M.G., Mukhamedzyanov, G.K. and Abdulagatov, I.M., 2011. Experimental study of the density and viscosity of polyethylene glycols and their mixtures at temperatures from 293 K to 473 K and at atmospheric pressure. *The Journal of Chemical Thermodynamics*, 43, pp.1824-1843.
- 30) Cocchi, M., Marchetti, A., Pigani, L., Sanna, G., Tassi, L., Ulrici, A., Vaccari, G. and Zanardi, C., 2000. Density and volumetric properties of ethane-1, 2-diol+ di-ethyleneglycol mixtures at different temperatures. *Fluid phase equilibria*, 172, pp.93-104.
- 31) Tawfik, W.Y. and Teja, A.S., 1989. The densities of polyethylene glycols. *Chemical engineering science*, 44, pp.921-923.
- 32) Klimaszewski, K., Stronka-Lewkowska, E., Abramczyk, K. and Bald, A., 2015. Acoustic and volumetric studies on (triethylene glycol+ water) mixtures in a wide temperature range. *The Journal of Chemical Thermodynamics*, 89, pp.212-222.

- 33) Valtz, A., Teodorescu, M., Wichterle, I. and Richon, D., 2004. Liquid densities and excess molar volumes for water+ diethylene glycolamine, and water, methanol, ethanol, 1-propanol+ triethylene glycol binary systems at atmospheric pressure and temperatures in the range of 283.15–363.15 K. *Fluid phase equilibria*, 215, pp.129-142.
- 34) Jayarathna, S.A., Kottage, D.A., Eimer, D.A. and Melaaen, M.C., 2012. Densities of partially carbonated aqueous diethanolamine and methyldiethanolamine solutions. *Journal of Chemical & Engineering Data*, 57, pp.2975-2984.
- 35) Wang, X., Kang, K., Wang, W. and Tian, Y., 2013. Volumetric properties of binary mixtures of 3-(methylamino) propylamine with water, N-methyldiethanolamine, N, N-dimethylethanolamine, and N, N-diethylethanolamine from (283.15 to 363.15) K. *Journal of Chemical & Engineering Data*, 58, pp.3430-3439.
- 36) Han, J., Jin, J., Eimer, D.A. and Melaaen, M.C., 2012. Density of Water (1)+ Diethanolamine (2)+ CO<sub>2</sub> (3) and Water (1)+ N-Methyldiethanolamine (2)+ CO<sub>2</sub> (3) from (298.15 to 423.15) K. *Journal of Chemical & Engineering Data*, 57, pp.1843-1850.
- 37) Guthrie Jr, G.B., Scott, D.W., Hubbard, W.N., Katz, C., McCullough, J.P., Gross, M.E., Williamson, K.D. and Waddington, G., 1952. Thermodynamic properties of furan. *Journal of the American Chemical Society*, 74, pp.4662-4669.
- 38) Timmermans, J., 1959. Work of the International Bureau of Physico-Chemical Standards-XI. Study of the physical constants of twenty organic compounds. *Journal of Physical Chemistry*, 56, pp. 984-1023.
- 39) Krakowiak, J., Koziel, H. and Grzybkowski, W., 2005. Apparent molar volumes of divalent transition metal perchlorates and chlorides in N, N-dimethylacetamide. *Journal of molecular liquids*, 118, pp.57-65.
- 40) Płaczek, A., Koziel, H. and Grzybkowski, W., 2007. Apparent molar compressibilities and volumes of some 1, 1-electrolytes in N, N-dimethylacetamide and N, N-dimethylformamide. *Journal of Chemical & Engineering Data*, 52, pp.699-706.
- 41) Warmińska, D., Fuchs, A. and Lundberg, D., 2013. Apparent molar volumes and compressibilities of lanthanum, gadolinium, lutetium and sodium trifluoromethanesulfonates in N, N-dimethylformamide and N, N-dimethylacetamide. *The Journal of Chemical Thermodynamics*, 58, pp.46-54.



42) Mejía, A., Segura, H., Cartes, M. and Coutinho, J.A., 2012. Vapor–liquid equilibrium, densities, and interfacial tensions of the system hexane+ 2, 5-dimethylfuran. *Journal of Chemical & Engineering Data*, 57, pp.2681-2688.

Table 1: Details of chemicals used in this work. All chemicals were used as received.

Product	abbreviations	CAS no.	chemical formula	purity ( <i>mass fraction, GC</i> )	source
furan	furan	110-00-9	C <sub>4</sub> H <sub>4</sub> O	≥ 0.99	Sigma - Aldrich
n-methyldiethanolamine	MDEA	105-59-9	CH <sub>3</sub> N(C <sub>2</sub> H <sub>4</sub> OH) <sub>2</sub>	0.99+	Arcos Organics
diethylene glycol	DEG	111-46-6	C <sub>4</sub> H <sub>10</sub> O <sub>3</sub>	0.99	Arcos Organics
triethylene glycol	TEG	112-27-6	C <sub>6</sub> H <sub>14</sub> O <sub>4</sub>	0.99	Arcos Organics
2-5-dimethylfuran	DMF	625-86-5	C <sub>6</sub> H <sub>8</sub> O	0.99	Sigma - Aldrich
n-n-dimethylacetamide	DMA	127-19-5	C <sub>4</sub> H <sub>9</sub> NO	≥ 0.99	Sigma - Aldrich

Table 2: Comparison between the experimental data measured in this work and those from literature for density values of pure components as a function of temperature T, at atmospheric pressure p = 100.65 kPa<sup>a</sup>

T/ K	$\rho/ \text{g.cm}^{-3}$		T/ K	$\rho/ \text{g.cm}^{-3}$		T/ K	$\rho/ \text{g.cm}^{-3}$	
	This work	Literature		This work	Literature		This work	Literature
DEG			TEG			MDEA		
278.16	1.12870		278.16	1.13815	1.13514 <sup>f</sup>	278.16	1.05141	
283.15	1.12512	1.12424 <sup>b</sup>	283.15	1.13423	1.13129 <sup>f</sup>	283.15	1.04767	
288.15	1.12152	1.12065 <sup>b</sup>	288.15	1.13029	1.12743 <sup>f</sup>	288.15	1.04385	
293.15	1.11793	1.11704 <sup>c</sup>	293.15	1.12638	1.12356 <sup>f</sup>	293.15	1.04010	1.03990 <sup>h</sup>
		1.11705 <sup>b</sup>			1.12369 <sup>g</sup>			1.04006 <sup>i</sup>
		1.11670 <sup>d</sup>						
298.15	1.11433	1.11402 <sup>c</sup>	298.15	1.12247	1.11969 <sup>f</sup>	298.15	1.03629	1.03600 <sup>j</sup>
		1.11347 <sup>b</sup>			1.11979 <sup>g</sup>			
		1.11350 <sup>d</sup>						
303.15	1.11072	1.11180 <sup>e</sup>	299.10		1.12120 <sup>e</sup>	303.15	1.03249	1.03240 <sup>h</sup>
		1.10988 <sup>b</sup>						1.03247 <sup>i</sup>
			303.15	1.11855	1.11581 <sup>f</sup>			1.03240 <sup>j</sup>
					1.11585 <sup>g</sup>			
Furan			DMA			DMF		
278.16	0.95856	0.95856 <sup>k</sup>	278.16	0.95551		278.16	0.91604	
283.15	0.95185	0.95144 <sup>l</sup>	283.15	0.95108	0.95006 <sup>n</sup>	283.15	0.91073	
		0.95185 <sup>k</sup>			0.95002 <sup>o</sup>			
					0.95004 <sup>p</sup>			
288.15	0.94508	0.94467 <sup>l</sup>	288.15	0.94627		288.15	0.90538	
		0.94508 <sup>k</sup>						
		0.93825 <sup>m</sup>						
293.15	0.93824	0.93781 <sup>l</sup>	293.15	0.94184	0.94085 <sup>n</sup>	293.15	0.90000	0.90118 <sup>q</sup>
		0.93824 <sup>k</sup>			0.94080 <sup>o</sup>			
					0.94083 <sup>p</sup>			
298.15	0.93133	0.93133 <sup>k</sup>	298.15	0.93703	0.93623 <sup>n</sup>	298.15	0.89460	
					0.93619 <sup>o</sup>			

					0.93622 <sup>p</sup>			
303.15	0.92437	0.92437 <sup>k</sup>	303.15	0.93260	0.93162 <sup>n</sup>	303.15	0.88917	0.89037 <sup>q</sup>
					0.93158 <sup>o</sup>			
					0.93161 <sup>p</sup>			
						308.15	0.88371	
			313.16	0.92334	0.92237 <sup>n</sup>	313.16	0.87822	0.87943 <sup>q</sup>
					0.92233 <sup>o</sup>			
					0.92235 <sup>p</sup>			
						318.16	0.87269	
			323.16	0.91406	0.91309 <sup>n</sup>	323.16	0.86713	0.86836 <sup>q</sup>
					0.91305 <sup>o</sup>			
					0.91308 <sup>p</sup>			
						328.16	0.86153	
			333.16	0.90475	0.90378 <sup>n</sup>	333.16	0.85588	0.85710 <sup>q</sup>
					0.90374 <sup>o</sup>			
					0.90376 <sup>p</sup>			
						338.16	0.85020	
			343.15	0.8954		343.15	0.84447	0.84567 <sup>q</sup>

<sup>a</sup> Standard uncertainty  $u(P) = 0.04$  kPa,  $u(T) = 0.012$  K. Expanded uncertainty (0.95 level of confidence,  $k=2$ )  $U(\rho) = 6 \times 10^{-4}$  g·cm<sup>-3</sup>. However, it is discussed elsewhere <sup>27</sup> that this uncertainty is optimistic, and the real uncertainty can be as low as 0.001 g·cm<sup>-3</sup>. <sup>b</sup> Reference 28, <sup>c</sup> Reference 29, <sup>d</sup> Reference 30, <sup>e</sup> Reference 31, <sup>f</sup> Reference 32, <sup>g</sup> 33, <sup>h</sup> Reference 34, <sup>i</sup> Reference 35, <sup>j</sup> Reference 36, <sup>k</sup> Reference 8, <sup>l</sup> Reference 37, <sup>m</sup> Reference 38, <sup>n</sup> Reference 39, <sup>o</sup> Reference 40, <sup>p</sup> Reference 41, <sup>q</sup> Reference 42.

Table 3: Experimental values of densities ( $\rho$ ) and excess molar volumes ( $V^E$ ) for the furan (1) + MDEA (2) binary system as a function of furan mole fraction  $x_1$  at atmospheric pressure  $p^a$ .

$x_1$	$d/\text{g}\cdot\text{cm}^{-3}$	$V^E/\text{cm}^3\cdot\text{mol}^{-1}$	$d/\text{g}\cdot\text{cm}^{-3}$	$V^E/\text{cm}^3\cdot\text{mol}^{-1}$	$d/\text{g}\cdot\text{cm}^{-3}$	$V^E/\text{cm}^3\cdot\text{mol}^{-1}$	$d/\text{g}\cdot\text{cm}^{-3}$	$V^E/\text{cm}^3\cdot\text{mol}^{-1}$	$d/\text{g}\cdot\text{cm}^{-3}$	$V^E/\text{cm}^3\cdot\text{mol}^{-1}$	$d/\text{g}\cdot\text{cm}^{-3}$	$V^E/\text{cm}^3\cdot\text{mol}^{-1}$
	T=278.15 K		T=283.15 K		T=288.15 K		T=293.15 K		T=298.15 K		T=303.15 K	
<sup>b</sup> 0.0000	1.05141	0.000	1.04767	0.000	1.04385	0.000	1.04010	0.000	1.03629	0.000	1.03249	0.000
0.1006	1.04729	-0.205	1.04333	-0.206	1.03934	-0.212	1.03538	-0.215	1.03140	-0.222	1.02741	-0.230
0.2258	1.04093	-0.385	1.03672	-0.392	1.03248	-0.404	1.02828	-0.415	1.02405	-0.430	1.01981	-0.445
0.3587	1.03253	-0.497	1.02804	-0.505	1.02352	-0.522	1.01902	-0.539	1.01449	-0.561	1.00996	-0.588
0.3966	1.02982	-0.516	1.02515	-0.521	1.02053	-0.538	1.01604	-0.567	1.01133	-0.581	1.00670	-0.605
0.5033	1.02112	-0.519	1.01617	-0.527	1.01129	-0.547	1.00653	-0.579	1.00154	-0.596	0.99673	-0.634
0.6001	1.01201	-0.486	1.00688	-0.503	1.00172	-0.524	0.99658	-0.548	0.99130	-0.566	0.98620	-0.605
0.6923	1.00214	-0.424	0.99674	-0.442	0.99127	-0.461	0.98583	-0.485	0.98024	-0.502	0.97483	-0.539
0.7920	0.98993	-0.319	0.98425	-0.341	0.97842	-0.357	0.97260	-0.377	0.96672	-0.399	0.96082	-0.422
0.8947	0.97572	-0.192	0.96952	-0.201	0.96325	-0.210	0.95698	-0.223	0.95064	-0.237	0.94425	-0.252
1.0000	0.95856	0.000	0.95185	0.000	0.94508	0.000	0.93824	0.000	0.93133	0.000	0.92437	0.000

<sup>a</sup> Standard uncertainty  $u(P) = 0.04$  kPa,  $u(T) = 0.012$  K. Expanded uncertainty (0.95 level of confidence,  $k=2$ )  $U(\rho) = 6 \times 10^{-4}$   $\text{g}\cdot\text{cm}^{-3}$ . <sup>b</sup> Reference 8

Table 4: Redlich–Kister parameters and deviations for the furan + MDEA binary system

T/ K	$a_0$	$a_1$	$a_2$	$a_3$	$a_4$	$a_5$	Variance/ $\sigma$
278.15	-2.091	0.289	0.139	-0.131	-0.350	-0.154	0.003
283.15	-2.124	0.205	-0.131	-0.106	0.020	-0.129	0.002
288.15	-2.204	0.183	-0.137	-0.140	0.030	-0.061	0.002
293.15	-2.322	0.174	0.054	-0.339	-0.218	0.104	0.002
298.15	-2.387	0.193	-0.119	-0.570	-0.076	0.317	0.001
303.15	-2.528	0.061	-0.056	-0.248	-0.100	0.030	0.002

Table 5: Experimental values of densities ( $\rho$ ) and excess molar volumes ( $V^E$ ) for the furan (1) + DEG (2) binary system as a function of furan mole fraction  $x_1$  at atmospheric pressure  $p^a$ .

$x_1$	$d/\text{g}\cdot\text{cm}^{-3}$	$V^E/\text{cm}^3\cdot\text{mol}^{-1}$	$d/\text{g}\cdot\text{cm}^{-3}$	$V^E/\text{cm}^3\cdot\text{mol}^{-1}$	$d/\text{g}\cdot\text{cm}^{-3}$	$V^E/\text{cm}^3\cdot\text{mol}^{-1}$	$d/\text{g}\cdot\text{cm}^{-3}$	$V^E/\text{cm}^3\cdot\text{mol}^{-1}$	$d/\text{g}\cdot\text{cm}^{-3}$	$V^E/\text{cm}^3\cdot\text{mol}^{-1}$	$d/\text{g}\cdot\text{cm}^{-3}$	$V^E/\text{cm}^3\cdot\text{mol}^{-1}$
	T=278.15 K		T=283.15 K		T=288.15 K		T=293.15 K		T=298.15 K		T=303.15 K	
<sup>b</sup> 0.0000	1.12870	0	1.12512	0	1.12152	0	1.11793	0	1.11433	0	1.11072	0
0.1006	1.11859	-0.258	1.11484	-0.270	1.11107	-0.282	1.10730	-0.295	1.10352	-0.309	1.09973	-0.323
0.1973	1.10761	-0.464	1.10366	-0.485	1.09970	-0.508	1.09573	-0.531	1.09174	-0.556	1.08775	-0.582
0.3257	1.09090	-0.609	1.08665	-0.638	1.08239	-0.669	1.07810	-0.701	1.07381	-0.736	1.06950	-0.772
0.4127	1.07824	-0.670	1.07376	-0.702	1.06925	-0.736	1.06473	-0.773	1.06019	-0.811	1.05563	-0.852
0.5174	1.06166	-0.702	1.05686	-0.736	1.05202	-0.771	1.04718	-0.809	1.04231	-0.851	1.03741	-0.893
0.6004	1.04702	-0.671	1.04193	-0.703	1.03682	-0.737	1.03168	-0.774	1.02652	-0.814	1.02132	-0.855
0.6978	1.02808	-0.571	1.02265	-0.600	1.01717	-0.630	1.01166	-0.662	1.00612	-0.697	1.00055	-0.734
0.7877	1.00937	-0.456	1.00358	-0.479	0.99775	-0.503	0.99187	-0.530	0.98596	-0.558	0.98001	-0.589
0.8729	0.99004	-0.297	0.98390	-0.312	0.97770	-0.328	0.97145	-0.346	0.96516	-0.366	0.95882	-0.386
1.0000	0.95856	0.000	0.95185	0.000	0.94508	0.000	0.93824	0.000	0.93133	0.000	0.92437	0.000

<sup>a</sup> Standard uncertainty  $u(P) = 0.04$  kPa,  $u(T) = 0.012$  K. Expanded uncertainty (0.95 level of confidence,  $k=2$ )  $U(\rho) = 6 \times 10^{-4}$   $\text{g}\cdot\text{cm}^{-3}$  (0.95 level of confidence).<sup>b</sup> Reference 8.

Table 6: Experimental values of densities ( $\rho$ ) and excess molar volumes ( $V^E$ ) for the furan (1) + TEG (2) binary system as a function of furan mole fraction  $x_1$  at atmospheric pressure  $p^a$ .

$x_1$	$d/\text{g}\cdot\text{cm}^{-3}$	$V^E/\text{cm}^3\cdot\text{mol}^{-1}$	$d/\text{g}\cdot\text{cm}^{-3}$	$V^E/\text{cm}^3\cdot\text{mol}^{-1}$	$d/\text{g}\cdot\text{cm}^{-3}$	$V^E/\text{cm}^3\cdot\text{mol}^{-1}$	$d/\text{g}\cdot\text{cm}^{-3}$	$V^E/\text{cm}^3\cdot\text{mol}^{-1}$	$d/\text{g}\cdot\text{cm}^{-3}$	$V^E/\text{cm}^3\cdot\text{mol}^{-1}$	$d/\text{g}\cdot\text{cm}^{-3}$	$V^E/\text{cm}^3\cdot\text{mol}^{-1}$
	T=278.15 K		T=283.15 K		T=288.15 K		T=293.15 K		T=298.15 K		T=303.15 K	
<sup>b</sup> 0.0000	1.13815	0.000	1.13423	0.000	1.13029	0.000	1.12638	0.000	1.12247	0.000	1.11855	0.000
0.1190	1.12936	-0.374	1.12529	-0.386	1.12121	-0.400	1.11717	-0.415	1.11316	-0.436	1.10910	-0.452
0.2221	1.12021	-0.632	1.11604	-0.658	1.11180	-0.680	1.10759	-0.704	1.10338	-0.731	1.09916	-0.758
0.3265	1.10918	-0.828	1.10482	-0.859	1.10042	-0.891	1.09605	-0.925	1.09165	-0.961	1.08725	-0.998
0.4293	1.09615	-0.942	1.09158	-0.979	1.08699	-1.017	1.08239	-1.056	1.07778	-1.098	1.07315	-1.142
0.5077	1.08466	-0.989	1.07990	-1.027	1.07510	-1.065	1.07032	-1.109	1.06550	-1.153	1.06068	-1.199
0.5940	1.06990	-0.972	1.06481	-1.002	1.05990	-1.053	1.05487	-1.095	1.04982	-1.142	1.04476	-1.190
0.6908	1.05049	-0.889	1.04510	-0.918	1.03997	-0.973	1.03452	-1.005	1.02947	-1.078	1.02390	-1.108
0.7890	1.02720	-0.736	1.02144	-0.759	1.01591	-0.806	1.01013	-0.836	1.00433	-0.871	0.99863	-0.919
0.9009	0.99466	-0.436	0.98811	-0.424	0.98197	-0.449	0.97588	-0.483	0.96940	-0.492	0.96357	-0.559
1.0000	0.95856	0.000	0.95185	0.000	0.94508	0.000	0.93824	0.000	0.93133	0.000	0.92437	0.000

<sup>a</sup> Standard uncertainty  $u(P) = 0.04$  kPa,  $u(T) = 0.012$  K. Expanded uncertainty (0.95 level of confidence,  $k=2$ )  $U(\rho) = 6 \times 10^{-4}$   $\text{g}\cdot\text{cm}^{-3}$  (0.95 level of confidence).<sup>b</sup>

Reference

8.



Table 7: Redlich–Kister parameters and deviations for the furan + DEG binary system

T/ K	$a_0$	$a_1$	$a_2$	$a_3$	$a_4$	$a_5$	Variance/ $\sigma$
278.15	-2.794	-0.065	0.290	0.840	-0.470	-0.974	0.004
283.15	-2.928	-0.069	0.279	0.823	-0.446	-0.940	0.005
288.15	-3.069	-0.071	0.289	0.818	-0.460	-0.928	0.005
293.15	-3.221	-0.079	0.297	0.808	-0.470	-0.920	0.005
298.15	-3.384	-0.095	0.311	0.815	-0.507	-0.947	0.005
303.15	-3.554	-0.113	0.316	0.820	-0.518	-0.955	0.005

Table 8: Redlich–Kister parameters and deviations for the furan + TEG binary system

T/ K	$a_0$	$a_1$	$a_2$	$a_3$	$a_4$	$a_5$	Variance/ $\sigma$
278.15	-3.930	-0.496	-0.115	-0.486	-0.528	-0.046	0.003
283.15	-4.070	-0.419	-0.270	-1.026	0.037	0.971	0.005
288.15	-4.236	-0.572	-0.511	-1.031	0.337	1.132	0.003
293.15	-4.409	-0.600	-0.285	-0.816	-0.229	0.487	0.003
298.15	-4.590	-0.810	-0.614	-0.473	0.411	0.644	0.006
303.15	-4.780	-0.806	-0.305	-0.434	-0.712	-0.338	0.003

Table 9: Experimental values of densities ( $\rho$ ) and excess molar volumes ( $V^E$ ) for the furan (1) + DMA (2) binary system as a function of furan mole fraction  $x_1$  at atmospheric pressure  $p^a$ .

$x_1$	$V^E$		$V^E$		$V^E$		$V^E$		$V^E$		$V^E$	
	$d/\text{g}\cdot\text{cm}^{-3}$	$/\text{cm}^3\cdot\text{mol}^{-1}$	$d/\text{g}\cdot\text{cm}^{-3}$	$/\text{cm}^3\cdot\text{mol}^{-1}$	$d/\text{g}\cdot\text{cm}^{-3}$	$/\text{cm}^3\cdot\text{mol}^{-1}$	$d/\text{g}\cdot\text{cm}^{-3}$	$/\text{cm}^3\cdot\text{mol}^{-1}$	$d/\text{g}\cdot\text{cm}^{-3}$	$/\text{cm}^3\cdot\text{mol}^{-1}$	$d/\text{g}\cdot\text{cm}^{-3}$	$/\text{cm}^3\cdot\text{mol}^{-1}$
	T=278.15 K		T=283.15 K		T=288.15 K		T=293.15 K		T=298.15 K		T=303.15 K	
<sup>b</sup> 0.0000	0.95551	0	0.95089	0	0.94627	0	0.94165	0	0.93703	0	0.93240	0
0.1487	0.96109	-0.478	0.95626	-0.487	0.95142	-0.495	0.94657	-0.504	0.94172	-0.514	0.93685	-0.523
0.2359	0.96370	-0.682	0.95874	-0.694	0.95375	-0.706	0.94876	-0.719	0.94375	-0.733	0.93874	-0.747
0.3254	0.96604	-0.850	0.96092	-0.864	0.95578	-0.880	0.95062	-0.896	0.94545	-0.914	0.94026	-0.932
0.4043	0.96715	-0.909	0.96190	-0.927	0.95661	-0.944	0.95130	-0.962	0.94598	-0.981	0.94063	-1.002
0.5076	0.96811	-0.940	0.96266	-0.959	0.95716	-0.977	0.95164	-0.996	0.94609	-1.017	0.94052	-1.039
0.5980	0.96819	-0.903	0.96254	-0.920	0.95684	-0.938	0.95112	-0.958	0.94536	-0.978	0.93958	-1.000
0.6891	0.96741	-0.796	0.96154	-0.812	0.95563	-0.828	0.94969	-0.846	0.94370	-0.865	0.93769	-0.884
0.7876	0.96568	-0.617	0.95958	-0.630	0.95342	-0.643	0.94721	-0.657	0.94096	-0.672	0.93467	-0.687
0.8758	0.96344	-0.408	0.95710	-0.417	0.95070	-0.426	0.94424	-0.435	0.93774	-0.446	0.93118	-0.456
1.0000	0.95856	0.000	0.95185	0.000	0.94508	0.000	0.93824	0.000	0.93133	0.000	0.92437	0.000

<sup>a</sup> Standard uncertainty  $u(P) = 0.04$  kPa,  $u(T) = 0.012$  K. Expanded uncertainty (0.95 level of confidence,  $k=2$ )  $U(\rho) = 6 \times 10^{-4}$   $\text{g}\cdot\text{cm}^{-3}$  (0.95 level of confidence).<sup>b</sup> Reference 8.

Table 10: Experimental values of densities ( $\rho$ ) and excess molar volumes ( $V^E$ ) for the DMF (1) + DMA (2) binary system as a function of furan mole fraction  $x_1$  at atmospheric pressure  $p^a$ .

$x_1$	T=283.15 K		T=293.15 K		T=303.15 K		T=313.15 K		T=323.15 K		T=333.15 K		T=343.15 K	
	$d/g.cm^{-3}$	$V^E/cm^3.mol^{-1}$	$d/g_3.cm^{-3}$	$V^E/cm^3.mo.l^{-1}$	$d/g.cm^{-3}$	$V^E/cm^3.m.ol^{-1}$	$d/g.cm^{-3}$	$V^E/cm^3.m.ol^{-1}$	$d/g_3.cm^{-3}$	$V^E/cm^3.mo.l^{-1}$	$d/g.cm^{-3}$	$V^E/cm^3.m.ol^{-1}$	$d/g.cm^{-3}$	$V^E/cm^3.m.ol^{-1}$
0.0000	0.95108	0.000	0.94184	0.000	0.93260	0.000	0.92334	0.000	0.91406	0.000	0.90475	0.000	0.89540	0.000
0.1280	0.94741	-0.213	0.93801	-0.225	0.92860	-0.237	0.91916	-0.250	0.90969	-0.265	0.90018	-0.281	0.89061	-0.299
0.2341	0.94413	-0.358	0.93460	-0.377	0.92505	-0.397	0.91545	-0.419	0.90581	-0.443	0.89612	-0.470	0.88636	-0.499
0.3157	0.94134	-0.435	0.93170	-0.458	0.92203	-0.483	0.91231	-0.510	0.90253	-0.540	0.89270	-0.573	0.88278	-0.609
0.4200	0.93762	-0.508	0.92783	-0.535	0.91800	-0.564	0.90811	-0.595	0.89816	-0.629	0.88813	-0.667	0.87801	-0.708
0.4919	0.93477	-0.523	0.92489	-0.552	0.91495	-0.582	0.90494	-0.615	0.89486	-0.651	0.88469	-0.690	0.87442	-0.732
0.6059	0.93005	-0.512	0.91998	-0.539	0.90985	-0.569	0.89964	-0.600	0.88935	-0.635	0.87895	-0.672	0.86844	-0.714
0.6823	0.92661	-0.465	0.91642	-0.490	0.90617	-0.517	0.89582	-0.546	0.88537	-0.577	0.87482	-0.611	0.86413	-0.649
0.7933	0.92143	-0.363	0.91108	-0.385	0.90063	-0.405	0.89007	-0.427	0.87940	-0.451	0.86861	-0.477	0.85766	-0.504
0.8823	0.91699	-0.235	0.90648	-0.248	0.89587	-0.262	0.88514	-0.276	0.87430	-0.291	0.86331	-0.308	0.85216	-0.325
1.0000	0.91073	0.000	0.90000	0.000	0.88917	0.000	0.87822	0.000	0.86713	0.000	0.85588	0.000	0.84447	0.000

<sup>a</sup> Standard uncertainty  $u(P) = 0.04$  kPa,  $u(T) = 0.012$  K. Expanded uncertainty (0.95 level of confidence,  $k=2$ )  $U(\rho) = 6 \times 10^{-4} g \cdot cm^{-3}$  (0.95 level of confidence).

Table 11: Redlich–Kister parameters and deviations for the furan + DMA binary system

T/ K	$a_0$	$a_1$	$a_2$	$a_3$	$a_4$	$a_5$	Variance/ $\sigma$
278.15	-3.772	0.141	0.003	0.124	0.126	-0.711	0.005
283.15	-3.846	0.137	0.034	0.081	0.050	-0.646	0.005
288.15	-3.919	0.130	0.038	0.078	0.047	-0.649	0.005
293.15	-3.997	0.120	0.035	0.078	0.053	-0.648	0.004
298.15	-4.080	0.105	0.035	0.091	0.043	-0.685	0.005
303.15	-4.166	0.096	0.035	0.079	0.051	-0.664	0.005

Table 12: Redlich–Kister parameters and deviations for the DMF + DMA binary system

T/ K	$a_0$	$a_1$	$a_2$	$a_3$	$a_4$	$a_5$	Variance/ $\sigma$
283.15	-2.095	-0.159	0.014	-0.113	0.000	-0.032	0.003
293.15	-2.208	-0.164	0.014	-0.203	-0.009	0.082	0.003
303.15	-2.328	-0.181	0.014	-0.167	-0.011	0.027	0.003
313.15	-2.460	-0.095	0.057	-0.972	-0.094	1.218	0.005
323.15	-2.601	-0.204	0.041	-0.134	-0.035	-0.024	0.003
333.15	-2.756	-0.211	0.046	-0.147	-0.031	-0.002	0.004
343.15	-2.927	-0.224	0.056	-0.102	-0.022	-0.057	0.004

Table 13: Experimental values of speed of sound  $c$  of each pure component studied as a function of temperature  $T$ , at atmospheric pressure  $p^a$ .

T/ K	DMF	DMA	MDEA	TEG	DEG
	$c/ \text{m.s}^{-1}$				
278.16	1278.05	1538.60	1632.85	1677.16	1632.74
283.15	1256.30	1518.29	1616.10	1661.79	1620.58
288.15	1234.27	1497.88	1599.06	1645.96	1608.35
293.15	1212.44	1477.69	1583.58	1631.23	1596.24
298.15	1190.61	1457.50	1567.52	1616.04	1584.08
303.15	1168.93	1437.48	1551.76	1601.00	1571.99
308.15	1147.37				
313.16	1125.94	1398.28			
318.16	1104.65				
323.16	1083.46	1359.11			
328.16	1062.40				
333.16	1041.47	1320.39			
338.16	1020.65				
343.15	999.90	1282.11			

<sup>a</sup> Standard uncertainty  $u(P) = 0.04$  kPa,  $u(T) = 0.012$  K. Expanded uncertainty (0.95 level of confidence,  $k=2$ )  $U(c) = 0.5 \text{ m.s}^{-1}$

Table 14: Values of the second-order polynomial expression (eq. 18) for MDEA <sup>a</sup>.

Property/ f	a	u(a)	b	u(b)	c	u(c)
$v/ \text{cm}^3.\text{mol}^{-1}$	8.09E-05	1E-05	0.0360	7E-03	97.1	1E+00
$\alpha/ \text{K}^{-1}$	-1.159E-09	8E-11	1.561E-06	5E-08	3.71E-04	7E-06
$C_p/ \text{J}.\text{mol}^{-1}.\text{K}^{-1}$	5.56E-05	5E-04	6.37E-01	4E-01	65.76	6E+01
$X_s$	3.07E-15	1E-15	3.06E-14	6E-13	1.10E-10	8E-11
$X_T$	3.143E-15	1E-18	2.637E-13	6E-16	1.054E-10	9E-14

<sup>a</sup> Standard uncertainty are  $u(Y)$  of parameter Y.

Table 15: Values of second-order polynomial expression (eq. 18) for DEG<sup>a</sup>.

Property/ f	a	u(a)	b	u(b)	c	u(c)
$v/ \text{cm}^3.\text{mol}^{-1}$	4.47E-05	1E-06	0.0349	6E-04	80.9	9E-02
$\alpha/ \text{K}^{-1}$	-6.444E-10	6E-12	9.056E-07	4E-09	4.34E-04	5E-07
$C_p/ \text{J}.\text{mol}^{-1}.\text{K}^{-1}$	-5.78E-04	8E-04	7.78E-01	5E-01	64.45	8E+01
$X_s$	3.01E-15	7E-17	-4.68E-13	4E-14	2.30E-10	6E-12
$X_T$	3.164E-15	4E-19	-3.757E-13	2E-16	2.368E-10	3E-14

<sup>a</sup> Standard uncertainty are  $u(Y)$  of parameter Y.

Table 16: Values of second-order polynomial expression (eq. 18) for TEG<sup>a</sup>.

Property/ f	a	u(a)	b	u(b)	c	u(c)
$v/ \text{cm}^3 \cdot \text{mol}^{-1}$	4.93E-05	4E-06	0.0639	2E-03	110.4	3E-01
$\alpha/ \text{K}^{-1}$	-4.361E-10	2E-11	5.109E-07	1E-08	5.83E-04	2E-06
$C_p/ \text{J} \cdot \text{mol}^{-1} \cdot \text{K}^{-1}$	3.71E-03	4E-04	-1.97E+00	3E-01	593.25	5E+01
$X_s$	3.14E-15	6E-16	-3.70E-13	3E-13	1.72E-10	5E-11
$X_T$	2.648E-15	1E-17	1.592E-13	6E-15	1.162E-10	8E-13

<sup>a</sup> Standard uncertainty are u(Y) of parameter Y.Table 17: Values of second-order polynomial expression (eq. 18) for DMA<sup>a</sup>.

Property/ f	a	u(a)	b	u(b)	c	u(c)
$v/ \text{cm}^3 \cdot \text{mol}^{-1}$	1.07E-04	2E-06	0.0276	1E-03	75.2	2E-01
$\alpha/ \text{K}^{-1}$	-2.417E-09	2E-11	2.780E-06	9E-09	3.72E-04	1E-06
$C_p/ \text{J} \cdot \text{mol}^{-1} \cdot \text{K}^{-1}$	1.31E-03	8E-05	-6.33E-01	5E-02	245.38	7E+00
$X_s$	1.54E-14	4E-16	-5.93E-12	2E-13	9.01E-10	4E-11
$X_T$	1.516E-14	4E-17	-4.825E-12	3E-14	7.482E-10	4E-12

<sup>a</sup> Standard uncertainty are u(Y) of parameter Y.Table 18: Values of second-order polynomial expression (eq. 18) for DMF<sup>a</sup>.

Property/ f	a	u(a)	b	u(b)	c	u(c)
$v/ \text{cm}^3 \cdot \text{mol}^{-1}$	2.55E-04	4E-06	-0.0219	3E-03	91.3	4E-01
$\alpha/ \text{K}^{-1}$	-6.804E-09	4E-11	7.336E-06	3E-08	-3.71E-04	4E-06
$C_p/ \text{J} \cdot \text{mol}^{-1} \cdot \text{K}^{-1}$	5.09E-04	2E-05	-1.96E-01	1E-02	89.70	2E+00
$X_s$	4.52E-14	1E-15	-2.02E-11	7E-13	2.79E-09	1E-10
$X_T$	5.446E-14	2E-16	-2.015E-11	1E-13	2.426E-09	2E-11

<sup>a</sup> Standard uncertainty are u(Y) of parameter Y.Table 19: Physical constants of pure compounds at 278.15 K, used for calculations of excess molar volume  $v^E$  with the PFP model:  $v_i^0$ , molar volume;  $\alpha_i$ , coefficient of thermal expansion;  $\chi_T$ , isothermal compressibility; reduction parameters of volume  $v_i^*$  and pressure  $p_i^*$ 

Compound	$V_i^0$ $\text{cm}^3 \cdot \text{mol}^{-1}$	$10^3 \times \alpha_i$ $\text{K}^{-1}$	$10^3 \times \chi_{T_i}$ $\text{MPa}^{-1}$	$V_i^*$ $\text{cm}^3 \cdot \text{mol}^{-1}$	$P_i^*$ $\text{MPa}$
furan	70.805	1.3925	1.0345	64.812	113.7464
MDEA	113.337	0.7152	0.4219	108.045	132.0577
DEG	94.019	0.6359	0.3771	90.082	130.0429
TEG	131.942	0.6917	0.3653	125.969	147.0802
DMA	91.179	0.9665	0.5810	85.579	133.6964



Table 20: Physical constants of pure compounds at 283.15 K, used for calculations of excess molar volume  $v^E$  with the PFP model:  $v_i^0$ , molar volume;  $\alpha_i$ , coefficient of thermal expansion;  $\chi_T$ , isothermal compressibility; reduction parameters of volume  $v_i^*$  and pressure  $p_i^*$

Compound	$V_i^0$ $cm^3.mol^{-1}$	$10^3 \times \alpha_i$ $K^{-1}$	$10^3 \times K_{Ti}$ $MPa^{-1}$	$V_i^*$ $cm^3.mol^{-1}$	$P_i^*$ $MPa$
furan	71.302	1.4173	1.0861	65.139	111.4807
MDEA	113.337	0.7198	0.4321	107.980	130.8534
DEG	94.319	0.6386	0.3841	90.328	129.2398
TEG	132.399	0.6930	0.3735	126.355	145.2505
DMA	91.621	0.9716	0.5994	85.933	131.3867
DMF	105.552	1.1611	1.0861	97.877	88.6522

Table 21: Physical constants of pure compounds at 288.15 K, used for calculations of excess molar volume  $v^E$  with the PFP model:  $v_i^0$ , molar volume;  $\alpha_i$ , coefficient of thermal expansion;  $\chi_T$ , isothermal compressibility; reduction parameters of volume  $v_i^*$  and pressure  $p_i^*$

Compound	$V_i^0$ $cm^3.mol^{-1}$	$10^3 \times \alpha_i$ $K^{-1}$	$10^3 \times K_{Ti}$ $MPa^{-1}$	$V_i^*$ $cm^3.mol^{-1}$	$P_i^*$ $MPa$
furan	71.811	1.4415	1.1407	65.551	107.3784
MDEA	113.337	0.7242	0.4424	107.984	127.6948
DEG	94.621	0.6413	0.3913	90.628	126.4919
TEG	132.860	0.6943	0.3819	126.824	141.2793
DMA	92.069	0.9766	0.6184	86.362	127.0845

Table 22: Physical constants of pure compounds at 293.15 K, used for calculations of excess molar volume  $v^E$  with the PFP model:  $v_i^0$ , molar volume;  $\alpha_i$ , coefficient of thermal expansion;  $\chi_T$ , isothermal compressibility; reduction parameters of volume  $v_i^*$  and pressure  $p_i^*$

Compound	$V_i^0$ $cm^3.mol^{-1}$	$10^3 \times \alpha_i$ $K^{-1}$	$10^3 \times K_{Ti}$ $MPa^{-1}$	$V_i^*$ $cm^3.mol^{-1}$	$P_i^*$ $MPa$
furan	72.331	1.4652	1.1982	65.899	105.0390
MDEA	113.337	0.7287	0.4528	107.919	126.5497
DEG	94.926	0.6439	0.3986	90.878	125.6734
TEG	133.321	0.6956	0.3904	127.214	139.5477
DMA	92.521	0.9815	0.6380	86.724	124.8408
DMF	106.811	1.1952	1.1981	98.844	83.0540

Table 23: Physical constants of pure compounds at 298.15 K, used for calculations of excess molar volume  $v^E$  with the PFP model:  $v_i^0$ , molar volume;  $\alpha_i$ , coefficient of thermal expansion;  $\chi_T$ , isothermal compressibility; reduction parameters of volume  $v_i^*$  and pressure  $p_i^*$

Compound	$V_i^0$ $cm^3.mol^{-1}$	$10^3 \times \alpha_i$ $K^{-1}$	$10^3 \times K_{Ti}$ $MPa^{-1}$	$V_i^*$ $cm^3.mol^{-1}$	$P_i^*$ $MPa$
furan	72.864	1.488	1.2584	66.337	101.0270
MDEA	113.337	0.733	0.4634	107.924	123.5142
DEG	95.233	0.647	0.4061	91.183	122.9687
TEG	133.786	0.697	0.3990	127.687	135.7621
DMA	92.977	0.986	0.6583	87.162	120.7175

Table 24: Physical constants of pure compounds at 303.15 K, used for calculations of excess molar volume  $v^E$  with the PFP model:  $v_i^o$ , molar volume;  $\alpha_i$ , coefficient of thermal expansion;  $\chi_T$ , isothermal compressibility; reduction parameters of volume  $v_i^*$  and pressure  $p_i^*$

Compound	$V_i^o$ $cm^3.mol^{-1}$	$10^3 \times \alpha_i$ $K^{-1}$	$10^3 \times K_{Ti}$ $MPa^{-1}$	$V_i^*$ $cm^3.mol^{-1}$	$P_i^*$ $MPa$
furan	73.411	1.5108	1.3216	66.711	98.7009
MDEA	113.337	0.7374	0.4742	107.859	122.4186
DEG	95.542	0.6491	0.4137	91.437	122.1437
TEG	134.254	0.6981	0.4077	128.085	134.1208
DMA	93.438	0.9910	0.6791	87.533	118.5615
DMF	108.112	1.2280	1.3215	99.855	77.6669

Table 25: Physical constants of pure compounds at 313.15 K, 323.15 K, 333.15 K, and 343.15 K used for calculations of excess molar volume  $v^E$  with the PFP model:  $v_i^o$ , molar volume;  $\alpha_i$ , coefficient of thermal expansion;  $\chi_T$ , isothermal compressibility; reduction parameters of volume  $v_i^*$  and pressure  $p_i^*$

T/ K	Compound	$V_i^o$ $cm^3.mol^{-1}$	$10^3 \times \alpha_i$ $K^{-1}$	$10^3 \times K_{Ti}$ $MPa^{-1}$	$V_i^*$ $cm^3.mol^{-1}$	$P_i^*$ $MPa$
313.15	DMA	109.460	1.2595	1.4560	100.966	71.9898
	DMF	94.355	1.0057	0.7242	88.351	112.1426
323.15	DMA	110.860	1.2896	1.6012	102.079	67.2581
	DMF	95.313	1.0181	0.7725	89.181	106.5898
333.15	DMA	112.317	1.3183	1.7571	103.249	62.8644
	DMF	96.294	1.0300	0.8238	90.034	101.2720
343.15	DMA	113.835	1.3455	1.9232	104.481	58.8022
	DMF	97.300	1.0415	0.8780	90.912	96.2048

Table 26: Calculated a, b and,  $X_{12}$  parameters used in the PFP theory

System	278.15 K			288.15 K			298.15 K		
	$X_{12}^o$	a	b	$X_{12}^o$	a	b	$X_{12}^o$	a	b
furan+MDEA	-1.38	-0.4877	-16.7345	6.61	1.2213	2.7483	14.10	1.0749	1.0462
furan+DEG	-21.96	1.0035	-1.1996	-13.56	1.0184	-1.8440	-5.06	1.0805	-4.6104
furan+TEG	-21.07	0.7743	-1.7737	-13.84	0.6753	-2.6732	-6.70	0.3941	-5.2562
furan+DMA	-75.53	0.9810	-0.4756	-69.62	0.9819	-0.4995	-63.91	0.9831	-0.5243

Table 27: Calculated a, b and,  $X_{12}$  parameters used in the PFP theory

System	283.15 K			293.15 K			303.15 K		
	$X_{12}^o$	a	b	$X_{12}^o$	a	b	$X_{12}^o$	a	b
furan+MDEA	2.78	1.5967	7.0378	9.97	1.1277	1.6778	17.05	1.0525	0.7835
furan+DEG	-17.87	1.0092	-1.4356	-9.27	1.0358	-2.6149	-0.81	1.5946	-27.9168
furan+TEG	-16.62	0.7023	-2.3925	-9.97	0.5774	-3.5686	-3.39	-0.0289	-9.1838
furan+DMA	-72.62	0.9815	-0.4865	-66.71	0.9824	-0.5126	-61.13	0.9837	-0.5392
DMF+DMA	-16.92	1.0251	-0.2235	-13.93	1.0315	-0.2719	-11.13	1.0416	-0.3472

Table 28: Calculated a, b and,  $X_{12}$  parameters used in the PFP theory for DMF + DMA

T/ K	$X_{12}^o$	a	b
313.15	-8.64	1.0571	-0.4624
323.15	-6.50	1.0811	-0.6370
333.15	-4.76	1.1187	-0.9075
343.15	-3.37	1.1807	-1.3469

Table 29: Evaluation of the different contributions of the PFP model for the furan(1) + MDEA(2) binary system at temperature range from T = 278.15 K to 303.15 K and comparison with experimental data

<b>278.15 K</b>												
x1	Calculated contribution			V <sup>E</sup>	V <sup>E</sup>	deviation	Calculated contribution with a, b			V <sup>E</sup>	V <sup>E</sup>	deviation
	Interactional	Free volume	P* effect	PFP	exp		Interactional	Free volume	P* effect	PFP	exp	
0.1006	-0.0027	-0.1315	-0.0130	-0.1472	-0.205	-0.058	-0.0379	-0.1315	-0.0130	-0.182	-0.205	-0.022
0.2258	-0.0058	-0.2694	-0.0267	-0.3019	-0.385	-0.083	-0.0666	-0.2694	-0.0267	-0.363	-0.385	-0.023
0.3587	-0.0087	-0.3789	-0.0377	-0.4252	-0.497	-0.072	-0.0715	-0.3789	-0.0377	-0.488	-0.497	-0.009
0.3966	-0.0094	-0.4020	-0.0400	-0.4514	-0.516	-0.064	-0.0678	-0.4020	-0.0400	-0.510	-0.516	-0.006
0.5033	-0.0110	-0.4450	-0.0444	-0.5004	-0.519	-0.019	-0.0453	-0.4450	-0.0444	-0.535	-0.519	0.015
0.6001	-0.0119	-0.4517	-0.0452	-0.5087	-0.486	0.022	-0.0111	-0.4517	-0.0452	-0.508	-0.486	0.021
0.6923	-0.0118	-0.4242	-0.0425	-0.4785	-0.424	0.054	0.0289	-0.4242	-0.0425	-0.438	-0.424	0.013
0.7920	-0.0105	-0.3501	-0.0351	-0.3957	-0.319	0.077	0.0686	-0.3501	-0.0351	-0.317	-0.319	-0.002
0.8947	-0.0069	-0.2152	-0.0216	-0.2438	-0.192	0.052	0.0793	-0.2152	-0.0216	-0.158	-0.192	-0.034
<b>283.15 K</b>												
0.1006	0.0055	-0.1404	-0.0182	-0.1532	-0.206	-0.052	-0.0252	-0.1404	-0.0182	-0.184	-0.206	-0.022
0.2258	0.0119	-0.2879	-0.0375	-0.3134	-0.392	-0.079	-0.0411	-0.2879	-0.0375	-0.366	-0.392	-0.026
0.3587	0.0179	-0.4052	-0.0528	-0.4401	-0.505	-0.065	-0.0370	-0.4052	-0.0528	-0.495	-0.505	-0.010
0.3966	0.0194	-0.4301	-0.0561	-0.4667	-0.521	-0.054	-0.0317	-0.4301	-0.0561	-0.518	-0.521	-0.003
0.5033	0.0228	-0.4764	-0.0622	-0.5158	-0.527	-0.011	-0.0073	-0.4764	-0.0622	-0.546	-0.527	0.019
0.6001	0.0246	-0.4841	-0.0633	-0.5228	-0.503	0.019	0.0249	-0.4841	-0.0633	-0.522	-0.503	0.019
0.6923	0.0246	-0.4551	-0.0596	-0.4901	-0.442	0.048	0.0598	-0.4551	-0.0596	-0.455	-0.442	0.013
0.7920	0.0218	-0.3761	-0.0493	-0.4036	-0.341	0.063	0.0906	-0.3761	-0.0493	-0.335	-0.341	-0.006
0.8947	0.0145	-0.2315	-0.0304	-0.2474	-0.201	0.046	0.0899	-0.2315	-0.0304	-0.172	-0.201	-0.029

<b>288.15 K</b>												
x1	Calculated contribution			V <sup>E</sup>	V <sup>E</sup>	deviation	Calculated contribution with a, b			V <sup>E</sup>	V <sup>E</sup>	deviation
	Interactional	Free volume	P* effect	PFP	exp		Interactional	Free volume	P* effect	PFP	exp	
0.1006	0.0133	-0.1492	-0.0246	-0.1606	-0.212	-0.051	-0.0159	-0.1492	-0.0246	-0.190	-0.212	-0.022
0.2258	0.0289	-0.3063	-0.0506	-0.3279	-0.404	-0.076	-0.0216	-0.3063	-0.0506	-0.379	-0.404	-0.025
0.3587	0.0437	-0.4316	-0.0714	-0.4593	-0.522	-0.063	-0.0089	-0.4316	-0.0714	-0.512	-0.522	-0.010
0.3966	0.0473	-0.4583	-0.0758	-0.4867	-0.538	-0.052	-0.0017	-0.4583	-0.0758	-0.536	-0.538	-0.003
0.5033	0.0558	-0.5082	-0.0841	-0.5365	-0.547	-0.011	0.0266	-0.5082	-0.0841	-0.566	-0.547	0.019
0.6001	0.0602	-0.5170	-0.0856	-0.5424	-0.524	0.019	0.0601	-0.5170	-0.0856	-0.542	-0.524	0.019
0.6923	0.0602	-0.4866	-0.0806	-0.5070	-0.461	0.046	0.0935	-0.4866	-0.0806	-0.474	-0.461	0.013
0.7920	0.0535	-0.4027	-0.0667	-0.4159	-0.357	0.059	0.1192	-0.4027	-0.0667	-0.350	-0.357	-0.006
0.8947	0.0357	-0.2484	-0.0411	-0.2538	-0.210	0.044	0.1080	-0.2484	-0.0411	-0.181	-0.210	-0.028
<b>293.15 K</b>												
0.1006	0.0205	-0.1580	-0.0321	-0.1696	-0.215	-0.045	-0.0072	-0.1580	-0.0321	-0.197	-0.215	-0.018
0.2258	0.0447	-0.3245	-0.0660	-0.3458	-0.415	-0.069	-0.0033	-0.3245	-0.0660	-0.394	-0.415	-0.021
0.3587	0.0676	-0.4579	-0.0932	-0.4835	-0.539	-0.056	0.0176	-0.4579	-0.0932	-0.534	-0.539	-0.006
0.3966	0.0733	-0.4864	-0.0990	-0.5121	-0.567	-0.055	0.0266	-0.4864	-0.0990	-0.559	-0.567	-0.008
0.5033	0.0866	-0.5401	-0.1099	-0.5635	-0.579	-0.016	0.0586	-0.5401	-0.1099	-0.592	-0.579	0.012
0.6001	0.0936	-0.5502	-0.1119	-0.5685	-0.548	0.020	0.0932	-0.5502	-0.1119	-0.569	-0.548	0.021
0.6923	0.0938	-0.5186	-0.1055	-0.5302	-0.485	0.046	0.1251	-0.5186	-0.1055	-0.499	-0.485	0.014
0.7920	0.0835	-0.4300	-0.0874	-0.4338	-0.377	0.057	0.1458	-0.4300	-0.0874	-0.371	-0.377	-0.005
0.8947	0.0560	-0.2658	-0.0539	-0.2637	-0.223	0.040	0.1248	-0.2658	-0.0539	-0.195	-0.223	-0.028

<b>298.15 K</b>												
x1	Calculated contribution			V <sup>E</sup>	V <sup>E</sup>	deviation	Calculated contribution with a, b			V <sup>E</sup>	V <sup>E</sup>	deviation
	Interactional	Free volume	P* effect	PFP	exp		Interactional	Free volume	P* effect	PFP	exp	
0.1006	0.0296	-0.1666	-0.0405	-0.1775	-0.222	-0.045	0.0046	-0.1666	-0.0405	-0.203	-0.222	-0.020
0.2258	0.0647	-0.3427	-0.0834	-0.3613	-0.430	-0.068	0.0212	-0.3427	-0.0834	-0.405	-0.430	-0.025
0.3587	0.0980	-0.4842	-0.1177	-0.5039	-0.561	-0.057	0.0525	-0.4842	-0.1177	-0.549	-0.561	-0.011
0.3966	0.1064	-0.5146	-0.1251	-0.5333	-0.581	-0.047	0.0638	-0.5146	-0.1251	-0.576	-0.581	-0.005
0.5033	0.1258	-0.5723	-0.1390	-0.5854	-0.596	-0.011	0.1001	-0.5723	-0.1390	-0.611	-0.596	0.015
0.6001	0.1363	-0.5837	-0.1416	-0.5890	-0.566	0.023	0.1355	-0.5837	-0.1416	-0.590	-0.566	0.023
0.6923	0.1369	-0.5511	-0.1335	-0.5477	-0.502	0.045	0.1650	-0.5511	-0.1335	-0.520	-0.502	0.017
0.7920	0.1222	-0.4578	-0.1106	-0.4462	-0.399	0.048	0.1787	-0.4578	-0.1106	-0.390	-0.399	-0.009
0.8947	0.0821	-0.2836	-0.0683	-0.2698	-0.237	0.032	0.1448	-0.2836	-0.0683	-0.207	-0.237	-0.030
<b>303.15 K</b>												
0.1006	0.0366	-0.1750	-0.0500	-0.1884	-0.230	-0.041	0.0133	-0.1750	-0.0500	-0.212	-0.230	-0.018
0.2258	0.0801	-0.3605	-0.1029	-0.3832	-0.445	-0.062	0.0395	-0.3605	-0.1029	-0.424	-0.445	-0.021
0.3587	0.1216	-0.5102	-0.1454	-0.5341	-0.588	-0.054	0.0790	-0.5102	-0.1454	-0.577	-0.588	-0.011
0.3966	0.1320	-0.5425	-0.1545	-0.5650	-0.605	-0.040	0.0921	-0.5425	-0.1545	-0.605	-0.605	0.000
0.5033	0.1564	-0.6042	-0.1718	-0.6197	-0.634	-0.014	0.1321	-0.6042	-0.1718	-0.644	-0.634	0.010
0.6001	0.1697	-0.6173	-0.1751	-0.6228	-0.605	0.018	0.1686	-0.6173	-0.1751	-0.624	-0.605	0.019
0.6923	0.1707	-0.5839	-0.1652	-0.5783	-0.539	0.039	0.1967	-0.5839	-0.1652	-0.552	-0.539	0.013
0.7920	0.1528	-0.4861	-0.1370	-0.4703	-0.422	0.048	0.2054	-0.4861	-0.1370	-0.418	-0.422	-0.004
0.8947	0.1030	-0.3019	-0.0847	-0.2836	-0.252	0.032	0.1617	-0.3019	-0.0847	-0.225	-0.252	-0.027

Table 30: Evaluation of the different contributions of the PFP model for the furan(1) + DEG(2) binary system at temperature range from T = 278.15 K to 303.15 K and comparison with experimental data

<b>278.15 K</b>												
x1	Calculated contribution			V <sup>E</sup>	V <sup>E</sup>	deviation	Calculated contribution with a, b			V <sup>E</sup>	V <sup>E</sup>	deviation
	Interactional	Free volume	P* effect	PFP	exp		Interactional	Free volume	P* effect	PFP	exp	
0.1006	-0.039	-0.173	0.012	-0.200	-0.258	-0.058	-0.079	-0.173	0.012	-0.241	-0.258	-0.017
0.1973	-0.075	-0.311	0.021	-0.366	-0.464	-0.099	-0.141	-0.311	0.021	-0.431	-0.464	-0.033
0.3257	-0.120	-0.448	0.031	-0.538	-0.609	-0.071	-0.194	-0.448	0.031	-0.612	-0.609	0.003
0.4127	-0.146	-0.508	0.035	-0.619	-0.670	-0.050	-0.210	-0.508	0.035	-0.683	-0.670	0.013
0.5174	-0.169	-0.541	0.037	-0.673	-0.702	-0.029	-0.203	-0.541	0.037	-0.707	-0.702	0.005
0.6004	-0.179	-0.535	0.037	-0.677	-0.671	0.006	-0.179	-0.535	0.037	-0.677	-0.671	0.006
0.6978	-0.177	-0.486	0.034	-0.629	-0.571	0.058	-0.132	-0.486	0.034	-0.584	-0.571	0.013
0.7877	-0.157	-0.398	0.028	-0.527	-0.456	0.070	-0.077	-0.398	0.028	-0.447	-0.456	-0.009
0.8729	-0.116	-0.273	0.019	-0.369	-0.297	0.072	-0.027	-0.273	0.019	-0.280	-0.297	-0.017
<b>283.15 K</b>												
0.1006	-0.032	-0.184	0.005	-0.212	-0.270	-0.058	-0.072	-0.184	0.005	-0.252	-0.270	-0.018
0.1973	-0.063	-0.332	0.009	-0.386	-0.485	-0.099	-0.128	-0.332	0.009	-0.451	-0.485	-0.034
0.3257	-0.100	-0.479	0.013	-0.567	-0.638	-0.072	-0.174	-0.479	0.013	-0.641	-0.638	0.003
0.4127	-0.122	-0.544	0.014	-0.651	-0.702	-0.051	-0.186	-0.544	0.014	-0.715	-0.702	0.014
0.5174	-0.141	-0.581	0.016	-0.706	-0.736	-0.030	-0.176	-0.581	0.016	-0.741	-0.736	0.005
0.6004	-0.150	-0.574	0.015	-0.709	-0.703	0.006	-0.151	-0.574	0.015	-0.710	-0.703	0.007
0.6978	-0.148	-0.523	0.014	-0.657	-0.600	0.057	-0.104	-0.523	0.014	-0.613	-0.600	0.013
0.7877	-0.132	-0.429	0.012	-0.549	-0.479	0.070	-0.053	-0.429	0.012	-0.470	-0.479	-0.009
0.8729	-0.098	-0.294	0.008	-0.384	-0.312	0.072	-0.009	-0.294	0.008	-0.295	-0.312	-0.017



<b>288.15 K</b>												
x1	Calculated contribution			V <sup>E</sup>	V <sup>E</sup>	deviation	Calculated contribution with a, b			V <sup>E</sup>	V <sup>E</sup>	deviation
	Interactional	Free volume	P* effect	PFP	exp		Interactional	Free volume	P* effect	PFP	exp	
0.1006	-0.025	-0.196	-0.003	-0.224	-0.282	-0.058	-0.065	-0.196	-0.003	-0.264	-0.282	-0.018
0.1973	-0.048	-0.353	-0.006	-0.407	-0.508	-0.100	-0.113	-0.353	-0.006	-0.473	-0.508	-0.035
0.3257	-0.078	-0.511	-0.009	-0.597	-0.669	-0.072	-0.152	-0.511	-0.009	-0.671	-0.669	0.002
0.4127	-0.095	-0.580	-0.010	-0.685	-0.736	-0.051	-0.159	-0.580	-0.010	-0.750	-0.736	0.014
0.5174	-0.110	-0.620	-0.011	-0.741	-0.771	-0.030	-0.146	-0.620	-0.011	-0.777	-0.771	0.006
0.6004	-0.117	-0.615	-0.011	-0.742	-0.737	0.005	-0.119	-0.615	-0.011	-0.744	-0.737	0.007
0.6978	-0.116	-0.561	-0.010	-0.687	-0.630	0.057	-0.073	-0.561	-0.010	-0.643	-0.630	0.014
0.7877	-0.104	-0.461	-0.008	-0.573	-0.503	0.070	-0.024	-0.461	-0.008	-0.494	-0.503	-0.009
0.8729	-0.077	-0.317	-0.006	-0.400	-0.328	0.072	0.013	-0.317	-0.006	-0.310	-0.328	-0.018
<b>293.15 K</b>												
0.1006	-0.017	-0.207	-0.013	-0.237	-0.295	-0.058	-0.057	-0.207	-0.013	-0.277	-0.295	-0.019
0.1973	-0.034	-0.374	-0.023	-0.430	-0.531	-0.101	-0.098	-0.374	-0.023	-0.495	-0.531	-0.036
0.3257	-0.054	-0.542	-0.033	-0.629	-0.701	-0.072	-0.129	-0.542	-0.033	-0.704	-0.701	0.002
0.4127	-0.066	-0.617	-0.038	-0.721	-0.773	-0.051	-0.131	-0.617	-0.038	-0.786	-0.773	0.013
0.5174	-0.077	-0.661	-0.041	-0.779	-0.809	-0.030	-0.113	-0.661	-0.041	-0.815	-0.809	0.006
0.6004	-0.082	-0.656	-0.041	-0.779	-0.774	0.005	-0.085	-0.656	-0.041	-0.782	-0.774	0.008
0.6978	-0.082	-0.600	-0.037	-0.719	-0.662	0.057	-0.039	-0.600	-0.037	-0.676	-0.662	0.015
0.7877	-0.073	-0.494	-0.031	-0.599	-0.530	0.069	0.006	-0.494	-0.031	-0.520	-0.530	-0.010
0.8729	-0.055	-0.341	-0.021	-0.417	-0.346	0.071	0.035	-0.341	-0.021	-0.327	-0.346	-0.018

<b>298.15 K</b>												
x1	Calculated contribution			V <sup>E</sup>	V <sup>E</sup>	deviation	Calculated contribution with a, b			V <sup>E</sup>	V <sup>E</sup>	deviation
	Interactional	Free volume	P* effect	PFP	exp		Interactional	Free volume	P* effect	PFP	exp	
0.1006	-0.010	-0.218	-0.023	-0.251	-0.309	-0.058	-0.049	-0.218	-0.023	-0.290	-0.309	-0.019
0.1973	-0.019	-0.395	-0.042	-0.455	-0.556	-0.101	-0.083	-0.395	-0.042	-0.519	-0.556	-0.037
0.3257	-0.030	-0.573	-0.061	-0.664	-0.736	-0.072	-0.104	-0.573	-0.061	-0.738	-0.736	0.002
0.4127	-0.037	-0.654	-0.069	-0.760	-0.811	-0.051	-0.102	-0.654	-0.069	-0.825	-0.811	0.013
0.5174	-0.043	-0.702	-0.075	-0.820	-0.851	-0.031	-0.080	-0.702	-0.075	-0.856	-0.851	0.006
0.6004	-0.046	-0.698	-0.074	-0.818	-0.814	0.005	-0.050	-0.698	-0.074	-0.822	-0.814	0.008
0.6978	-0.046	-0.640	-0.068	-0.754	-0.697	0.057	-0.004	-0.640	-0.068	-0.712	-0.697	0.015
0.7877	-0.041	-0.529	-0.056	-0.626	-0.558	0.068	0.036	-0.529	-0.056	-0.549	-0.558	-0.010
0.8729	-0.031	-0.365	-0.039	-0.435	-0.366	0.070	0.058	-0.365	-0.039	-0.346	-0.366	-0.019
<b>303.15 K</b>												
0.1006	-0.002	-0.229	-0.034	-0.265	-0.323	-0.058	-0.040	-0.229	-0.034	-0.304	-0.323	-0.019
0.1973	-0.003	-0.415	-0.062	-0.481	-0.582	-0.101	-0.066	-0.415	-0.062	-0.544	-0.582	-0.038
0.3257	-0.005	-0.604	-0.091	-0.700	-0.772	-0.071	-0.078	-0.604	-0.091	-0.774	-0.772	0.002
0.4127	-0.006	-0.690	-0.104	-0.801	-0.852	-0.051	-0.070	-0.690	-0.104	-0.865	-0.852	0.013
0.5174	-0.007	-0.743	-0.112	-0.862	-0.893	-0.031	-0.044	-0.743	-0.112	-0.899	-0.893	0.006
0.6004	-0.008	-0.740	-0.112	-0.860	-0.855	0.005	-0.012	-0.740	-0.112	-0.864	-0.855	0.009
0.6978	-0.008	-0.680	-0.103	-0.791	-0.734	0.057	0.033	-0.680	-0.103	-0.750	-0.734	0.016
0.7877	-0.007	-0.564	-0.085	-0.656	-0.589	0.067	0.070	-0.564	-0.085	-0.579	-0.589	-0.010
0.8729	-0.005	-0.391	-0.059	-0.455	-0.386	0.069	0.084	-0.391	-0.059	-0.366	-0.386	-0.020

Table 31: Evaluation of the different contributions of the PFP model for the furan(1) + TEG(2) binary system at temperature range from T = 278.15 K to 303.15 K and comparison with experimental data.

<b>278.15 K</b>												
$x_1$	Calculated contribution			$V^E$	$V^E$	deviation	Calculated contribution with a, b			$V^E$	$V^E$	deviation
	Interactional	Free volume	P* effect	PFP	exp		Interactional	Free volume	P* effect	PFP	exp	
0.1190	-0.0417	-0.1535	-0.0949	-0.2901	-0.374	-0.084	0.1190	-0.0972	-0.1535	-0.0949	-0.346	-0.374
0.2221	-0.0761	-0.2711	-0.1670	-0.5141	-0.632	-0.117	0.2221	-0.1612	-0.2711	-0.1670	-0.599	-0.632
0.3265	-0.1083	-0.3724	-0.2282	-0.7088	-0.828	-0.119	0.3265	-0.2033	-0.3724	-0.2282	-0.804	-0.828
0.4293	-0.1361	-0.4500	-0.2742	-0.8603	-0.942	-0.082	0.4293	-0.2185	-0.4500	-0.2742	-0.943	-0.942
0.5077	-0.1534	-0.4907	-0.2975	-0.9415	-0.989	-0.047	0.5077	-0.2104	-0.4907	-0.2975	-0.999	-0.989
0.5940	-0.1666	-0.5123	-0.3086	-0.9875	-0.972	0.016	0.5940	-0.1805	-0.5123	-0.3086	-1.001	-0.972
0.6908	-0.1710	-0.4997	-0.2985	-0.9691	-0.889	0.080	0.6908	-0.1215	-0.4997	-0.2985	-0.920	-0.889
0.7890	-0.1575	-0.4341	-0.2567	-0.8482	-0.736	0.112	0.7890	-0.0423	-0.4341	-0.2567	-0.733	-0.736
0.9009	-0.1050	-0.2678	-0.1560	-0.5288	-0.436	0.093	0.9009	0.0356	-0.2678	-0.1560	-0.388	-0.436
<b>283.15 K</b>												
0.1190	-0.0336	-0.1659	-0.1010	-0.3005	-0.386	-0.085	-0.0942	-0.1659	-0.1010	-0.361	-0.386	-0.025
0.2221	-0.0614	-0.2932	-0.1777	-0.5322	-0.658	-0.126	-0.1546	-0.2932	-0.1777	-0.625	-0.658	-0.033
0.3265	-0.0875	-0.4028	-0.2428	-0.7332	-0.859	-0.126	-0.1918	-0.4028	-0.2428	-0.837	-0.859	-0.022
0.4293	-0.1102	-0.4869	-0.2919	-0.8890	-0.979	-0.090	-0.2011	-0.4869	-0.2919	-0.980	-0.979	0.001
0.5077	-0.1244	-0.5311	-0.3167	-0.9723	-1.027	-0.055	-0.1877	-0.5311	-0.3167	-1.036	-1.027	0.009
0.5940	-0.1354	-0.5547	-0.3287	-1.0188	-1.002	0.017	-0.1516	-0.5547	-0.3287	-1.035	-1.002	0.033
0.6908	-0.1392	-0.5414	-0.3180	-0.9986	-0.918	0.081	-0.0859	-0.5414	-0.3180	-0.945	-0.918	0.028
0.7890	-0.1286	-0.4707	-0.2735	-0.8728	-0.759	0.114	-0.0027	-0.4707	-0.2735	-0.747	-0.759	-0.012
0.9009	-0.0861	-0.2906	-0.1663	-0.5431	-0.424	0.119	0.0688	-0.2906	-0.1663	-0.388	-0.424	-0.036

<b>288.15 K</b>												
$x_1$	Calculated contribution			$V^E$	$V^E$	deviation	Calculated contribution with a, b			$V^E$	$V^E$	deviation
	Interactional	Free volume	P* effect	PFP	exp		Interactional	Free volume	P* effect	PFP	exp	
0.1190	-0.0286	-0.1785	-0.1082	-0.3153	-0.400	-0.084	-0.0865	-0.1785	-0.1082	-0.373	-0.400	-0.027
0.2221	-0.0523	-0.3155	-0.1904	-0.5582	-0.680	-0.122	-0.1415	-0.3155	-0.1904	-0.647	-0.680	-0.033
0.3265	-0.0747	-0.4336	-0.2603	-0.7687	-0.891	-0.122	-0.1747	-0.4336	-0.2603	-0.869	-0.891	-0.022
0.4293	-0.0942	-0.5245	-0.3129	-0.9317	-1.017	-0.086	-0.1818	-0.5245	-0.3129	-1.019	-1.017	0.002
0.5077	-0.1065	-0.5723	-0.3397	-1.0185	-1.065	-0.047	-0.1680	-0.5723	-0.3397	-1.080	-1.065	0.015
0.5940	-0.1162	-0.5981	-0.3526	-1.0669	-1.053	0.014	-0.1326	-0.5981	-0.3526	-1.083	-1.053	0.031
0.6908	-0.1197	-0.5842	-0.3413	-1.0452	-0.973	0.072	-0.0695	-0.5842	-0.3413	-0.995	-0.973	0.022
0.7890	-0.1109	-0.5084	-0.2938	-0.9130	-0.806	0.107	0.0095	-0.5084	-0.2938	-0.793	-0.806	-0.014
0.9009	-0.0746	-0.3144	-0.1787	-0.5677	-0.449	0.119	0.0747	-0.3144	-0.1787	-0.418	-0.449	-0.031
<b>293.15 K</b>												
0.1190	-0.0211	-0.1911	-0.1165	-0.3286	-0.415	-0.086	-0.0781	-0.1911	-0.1165	-0.386	-0.415	-0.029
0.2221	-0.0386	-0.3380	-0.2050	-0.5816	-0.704	-0.123	-0.1267	-0.3380	-0.2050	-0.670	-0.704	-0.035
0.3265	-0.0552	-0.4648	-0.2804	-0.8004	-0.925	-0.125	-0.1543	-0.4648	-0.2804	-0.900	-0.925	-0.026
0.4293	-0.0697	-0.5625	-0.3373	-0.9695	-1.056	-0.087	-0.1569	-0.5625	-0.3373	-1.057	-1.056	0.000
0.5077	-0.0789	-0.6142	-0.3662	-1.0593	-1.109	-0.049	-0.1405	-0.6142	-0.3662	-1.121	-1.109	0.012
0.5940	-0.0862	-0.6423	-0.3803	-1.1088	-1.095	0.013	-0.1034	-0.6423	-0.3803	-1.126	-1.095	0.031
0.6908	-0.0890	-0.6280	-0.3683	-1.0854	-1.005	0.081	-0.0402	-0.6280	-0.3683	-1.036	-1.005	0.032
0.7890	-0.0827	-0.5472	-0.3172	-0.9471	-0.836	0.111	0.0363	-0.5472	-0.3172	-0.828	-0.836	-0.008
0.9009	-0.0558	-0.3390	-0.1932	-0.5880	-0.483	0.105	0.0928	-0.3390	-0.1932	-0.439	-0.483	-0.044

<b>298.15 K</b>												
$x_1$	Calculated contribution			$V^E$	$V^E$	deviation	Calculated contribution with a, b			$V^E$	$V^E$	deviation
	Interactional	Free volume	P* effect	PFP	exp		Interactional	Free volume	P* effect	PFP	exp	
0.1190	-0.0145	-0.2038	-0.1257	-0.3440	-0.436	-0.092	-0.0724	-0.2038	-0.1257	-0.402	-0.436	-0.034
0.2221	-0.0265	-0.3606	-0.2213	-0.6085	-0.731	-0.122	-0.1162	-0.3606	-0.2213	-0.698	-0.731	-0.033
0.3265	-0.0380	-0.4963	-0.3029	-0.8371	-0.961	-0.124	-0.1392	-0.4963	-0.3029	-0.938	-0.961	-0.023
0.4293	-0.0481	-0.6011	-0.3644	-1.0135	-1.098	-0.085	-0.1374	-0.6011	-0.3644	-1.103	-1.098	0.004
0.5077	-0.0545	-0.6567	-0.3958	-1.1070	-1.153	-0.046	-0.1181	-0.6567	-0.3958	-1.171	-1.153	0.018
0.5940	-0.0596	-0.6874	-0.4112	-1.1583	-1.142	0.016	-0.0782	-0.6874	-0.4112	-1.177	-1.142	0.035
0.6908	-0.0618	-0.6729	-0.3985	-1.1331	-1.078	0.055	-0.0128	-0.6729	-0.3985	-1.084	-1.078	0.007
0.7890	-0.0576	-0.5871	-0.3434	-0.9881	-0.871	0.117	0.0635	-0.5871	-0.3434	-0.867	-0.871	-0.004
0.9009	-0.0390	-0.3645	-0.2094	-0.6129	-0.492	0.121	0.1133	-0.3645	-0.2094	-0.461	-0.492	-0.032
<b>303.15 K</b>												
0.1190	-0.0075	-0.2164	-0.1360	-0.3599	-0.452	-0.092	-0.0601	-0.2164	-0.1360	-0.413	-0.452	-0.039
0.2221	-0.0137	-0.3832	-0.2396	-0.6366	-0.758	-0.122	-0.0952	-0.3832	-0.2396	-0.718	-0.758	-0.040
0.3265	-0.0197	-0.5278	-0.3280	-0.8755	-0.998	-0.123	-0.1119	-0.5278	-0.3280	-0.968	-0.998	-0.030
0.4293	-0.0250	-0.6399	-0.3948	-1.0596	-1.142	-0.083	-0.1067	-0.6399	-0.3948	-1.141	-1.142	-0.001
0.5077	-0.0283	-0.6996	-0.4290	-1.1569	-1.199	-0.042	-0.0869	-0.6996	-0.4290	-1.215	-1.199	0.016
0.5940	-0.0311	-0.7330	-0.4459	-1.2100	-1.190	0.020	-0.0488	-0.7330	-0.4459	-1.228	-1.190	0.037
0.6908	-0.0322	-0.7185	-0.4324	-1.1831	-1.108	0.075	0.0115	-0.7185	-0.4324	-1.139	-1.108	0.031
0.7890	-0.0301	-0.6280	-0.3730	-1.0310	-0.919	0.112	0.0797	-0.6280	-0.3730	-0.921	-0.919	0.002
0.9009	-0.0205	-0.3908	-0.2277	-0.6390	-0.559	0.080	0.1188	-0.3908	-0.2277	-0.500	-0.559	-0.059

Table 32: Evaluation of the different contributions of the PFP model for the furan(1) + DMA(2) binary system at temperature range from T = 278.15 K to 303.15 K and comparison with experimental data

<b>278.15 K</b>												
x1	Calculated contribution			V <sup>E</sup>	V <sup>E</sup>	deviation	Calculated contribution with a, b			V <sup>E</sup>	V <sup>E</sup>	deviation
	Interactional	Free volume	P* effect	PFP	exp		Interactional	Free volume	P* effect	PFP	exp	
0.1487	-0.268	-0.062	-0.048	-0.377	-0.478	-0.101	-0.361	-0.062	-0.048	-0.471	-0.478	-0.007
0.2359	-0.402	-0.092	-0.070	-0.564	-0.682	-0.118	-0.516	-0.092	-0.070	-0.677	-0.682	-0.005
0.3254	-0.519	-0.116	-0.088	-0.723	-0.850	-0.127	-0.627	-0.116	-0.088	-0.831	-0.850	-0.019
0.4043	-0.600	-0.132	-0.099	-0.831	-0.909	-0.078	-0.685	-0.132	-0.099	-0.916	-0.909	0.007
0.5076	-0.669	-0.143	-0.107	-0.920	-0.940	-0.021	-0.701	-0.143	-0.107	-0.952	-0.940	0.012
0.5980	-0.687	-0.144	-0.107	-0.938	-0.903	0.035	-0.661	-0.144	-0.107	-0.912	-0.903	0.009
0.6891	-0.657	-0.134	-0.099	-0.890	-0.796	0.094	-0.571	-0.134	-0.099	-0.804	-0.796	0.008
0.7876	-0.555	-0.110	-0.081	-0.746	-0.617	0.130	-0.423	-0.110	-0.081	-0.614	-0.617	-0.003
0.8758	-0.389	-0.075	-0.055	-0.519	-0.408	0.111	-0.257	-0.075	-0.055	-0.387	-0.408	-0.021
<b>283.15 K</b>												
0.1487	-0.265	-0.069	-0.050	-0.384	-0.487	-0.103	-0.360	-0.069	-0.050	-0.479	-0.487	-0.008
0.2359	-0.399	-0.102	-0.073	-0.574	-0.694	-0.120	-0.514	-0.102	-0.073	-0.689	-0.694	-0.005
0.3254	-0.515	-0.128	-0.092	-0.736	-0.864	-0.129	-0.626	-0.128	-0.092	-0.846	-0.864	-0.018
0.4043	-0.596	-0.146	-0.104	-0.846	-0.927	-0.080	-0.683	-0.146	-0.104	-0.933	-0.927	0.007
0.5076	-0.666	-0.159	-0.112	-0.937	-0.959	-0.022	-0.700	-0.159	-0.112	-0.970	-0.959	0.012
0.5980	-0.685	-0.159	-0.112	-0.956	-0.920	0.036	-0.659	-0.159	-0.112	-0.930	-0.920	0.010
0.6891	-0.656	-0.148	-0.104	-0.908	-0.812	0.096	-0.569	-0.148	-0.104	-0.820	-0.812	0.008
0.7876	-0.555	-0.122	-0.084	-0.762	-0.630	0.132	-0.421	-0.122	-0.084	-0.627	-0.630	-0.003
0.8758	-0.390	-0.083	-0.057	-0.530	-0.417	0.113	-0.255	-0.083	-0.057	-0.395	-0.417	-0.022

<b>288.15 K</b>												
x1	Calculated contribution			V <sup>E</sup>	V <sup>E</sup>	deviation	Calculated contribution with a, b			V <sup>E</sup>	V <sup>E</sup>	deviation
	Interactional	Free volume	P* effect	PFP	exp		Interactional	Free volume	P* effect	PFP	exp	
0.1487	-0.262	-0.076	-0.052	-0.390	-0.495	-0.105	-0.359	-0.076	-0.052	-0.487	-0.495	-0.009
0.2359	-0.395	-0.112	-0.077	-0.583	-0.706	-0.123	-0.512	-0.112	-0.077	-0.701	-0.706	-0.005
0.3254	-0.510	-0.141	-0.097	-0.748	-0.880	-0.132	-0.623	-0.141	-0.097	-0.861	-0.880	-0.019
0.4043	-0.591	-0.161	-0.109	-0.861	-0.944	-0.083	-0.681	-0.161	-0.109	-0.950	-0.944	0.007
0.5076	-0.661	-0.175	-0.118	-0.954	-0.977	-0.023	-0.696	-0.175	-0.118	-0.989	-0.977	0.012
0.5980	-0.681	-0.175	-0.118	-0.974	-0.938	0.036	-0.655	-0.175	-0.118	-0.948	-0.938	0.010
0.6891	-0.653	-0.163	-0.109	-0.925	-0.828	0.097	-0.564	-0.163	-0.109	-0.837	-0.828	0.009
0.7876	-0.554	-0.134	-0.089	-0.777	-0.643	0.134	-0.417	-0.134	-0.089	-0.640	-0.643	-0.003
0.8758	-0.389	-0.092	-0.060	-0.541	-0.426	0.115	-0.251	-0.092	-0.060	-0.403	-0.426	-0.023
<b>293.15 K</b>												
0.1487	-0.259	-0.083	-0.055	-0.397	-0.504	-0.107	-0.357	-0.083	-0.055	-0.495	-0.504	-0.009
0.2359	-0.390	-0.122	-0.081	-0.594	-0.719	-0.125	-0.510	-0.122	-0.081	-0.714	-0.719	-0.006
0.3254	-0.505	-0.155	-0.102	-0.762	-0.896	-0.134	-0.620	-0.155	-0.102	-0.878	-0.896	-0.019
0.4043	-0.586	-0.176	-0.116	-0.877	-0.962	-0.085	-0.677	-0.176	-0.116	-0.969	-0.962	0.007
0.5076	-0.656	-0.191	-0.125	-0.972	-0.996	-0.024	-0.693	-0.191	-0.125	-1.009	-0.996	0.012
0.5980	-0.677	-0.192	-0.125	-0.994	-0.958	0.036	-0.651	-0.192	-0.125	-0.968	-0.958	0.010
0.6891	-0.650	-0.179	-0.116	-0.944	-0.846	0.098	-0.560	-0.179	-0.116	-0.855	-0.846	0.009
0.7876	-0.552	-0.147	-0.094	-0.793	-0.657	0.137	-0.412	-0.147	-0.094	-0.654	-0.657	-0.003
0.8758	-0.389	-0.100	-0.064	-0.553	-0.435	0.118	-0.248	-0.100	-0.064	-0.412	-0.435	-0.023

<b>298.15 K</b>												
x1	Calculated contribution			V <sup>E</sup>	V <sup>E</sup>	deviation	Calculated contribution with a, b			V <sup>E</sup>	V <sup>E</sup>	deviation
	Interactional	Free volume	P* effect	PFP	exp		Interactional	Free volume	P* effect	PFP	exp	
0.1487	-0.256	-0.090	-0.059	-0.405	-0.514	-0.109	-0.355	-0.090	-0.059	-0.504	-0.514	-0.010
0.2359	-0.386	-0.133	-0.087	-0.605	-0.733	-0.128	-0.507	-0.133	-0.087	-0.727	-0.733	-0.006
0.3254	-0.500	-0.168	-0.109	-0.777	-0.914	-0.136	-0.617	-0.168	-0.109	-0.895	-0.914	-0.019
0.4043	-0.581	-0.191	-0.123	-0.895	-0.981	-0.087	-0.674	-0.191	-0.123	-0.988	-0.981	0.007
0.5076	-0.651	-0.208	-0.133	-0.992	-1.017	-0.025	-0.689	-0.208	-0.133	-1.030	-1.017	0.013
0.5980	-0.673	-0.209	-0.133	-1.015	-0.978	0.036	-0.648	-0.209	-0.133	-0.989	-0.978	0.011
0.6891	-0.647	-0.195	-0.123	-0.965	-0.865	0.100	-0.556	-0.195	-0.123	-0.874	-0.865	0.009
0.7876	-0.551	-0.160	-0.100	-0.811	-0.672	0.139	-0.409	-0.160	-0.100	-0.669	-0.672	-0.003
0.8758	-0.388	-0.109	-0.068	-0.566	-0.446	0.119	-0.244	-0.109	-0.068	-0.422	-0.446	-0.024
<b>303.15 K</b>												
0.1487	-0.252	-0.097	-0.063	-0.413	-0.523	-0.111	-0.353	-0.097	-0.063	-0.514	-0.523	-0.010
0.2359	-0.381	-0.144	-0.092	-0.617	-0.747	-0.130	-0.505	-0.144	-0.092	-0.741	-0.747	-0.006
0.3254	-0.494	-0.182	-0.116	-0.793	-0.932	-0.139	-0.614	-0.182	-0.116	-0.912	-0.932	-0.019
0.4043	-0.575	-0.207	-0.132	-0.913	-1.002	-0.089	-0.670	-0.207	-0.132	-1.008	-1.002	0.007
0.5076	-0.645	-0.225	-0.142	-1.013	-1.039	-0.026	-0.685	-0.225	-0.142	-1.052	-1.039	0.013
0.5980	-0.668	-0.226	-0.142	-1.036	-1.000	0.036	-0.643	-0.226	-0.142	-1.011	-1.000	0.011
0.6891	-0.643	-0.211	-0.132	-0.985	-0.884	0.101	-0.551	-0.211	-0.132	-0.894	-0.884	0.009
0.7876	-0.548	-0.174	-0.107	-0.829	-0.687	0.141	-0.403	-0.174	-0.107	-0.684	-0.687	-0.003
0.8758	-0.387	-0.119	-0.073	-0.578	-0.456	0.122	-0.240	-0.119	-0.073	-0.431	-0.456	-0.025



Table 33: Evaluation of the different contributions of the PFP model for the DMF (1) + DMA(2) binary system at temperature range from T = 283.15 K to 343.15 K and comparison with experimental data

<b>283.15 K</b>												
x1	Calculated contribution			V <sup>E</sup>	V <sup>E</sup>	deviation	Calculated contribution with a, b			V <sup>E</sup>	V <sup>E</sup>	deviation
	Interactional	Free volume	P* effect	PFP	exp		Interactional	Free volume	P* effect	PFP	exp	
0.1280	-0.081	-0.015	-0.108	-0.204	-0.213	-0.010	-0.096	-0.015	-0.108	-0.219	-0.213	0.005
0.2341	-0.136	-0.026	-0.177	-0.339	-0.358	-0.019	-0.154	-0.026	-0.177	-0.357	-0.358	-0.001
0.3157	-0.170	-0.033	-0.217	-0.420	-0.435	-0.015	-0.187	-0.033	-0.217	-0.437	-0.435	0.001
0.4200	-0.202	-0.039	-0.251	-0.492	-0.508	-0.016	-0.212	-0.039	-0.251	-0.501	-0.508	-0.007
0.4909	-0.214	-0.042	-0.262	-0.518	-0.519	-0.001	-0.218	-0.042	-0.262	-0.521	-0.519	0.002
0.6059	-0.217	-0.043	-0.257	-0.516	-0.512	0.005	-0.209	-0.043	-0.257	-0.509	-0.512	-0.002
0.6823	-0.205	-0.040	-0.238	-0.483	-0.465	0.018	-0.191	-0.040	-0.238	-0.469	-0.465	0.004
0.7933	-0.164	-0.033	-0.185	-0.382	-0.363	0.019	-0.145	-0.033	-0.185	-0.363	-0.363	0.000
0.8823	-0.109	-0.022	-0.120	-0.251	-0.235	0.016	-0.092	-0.022	-0.120	-0.234	-0.235	-0.001
<b>293.15 K</b>												
0.1280	-0.071	-0.019	-0.125	-0.214	-0.225	-0.011	-0.087	-0.019	-0.125	-0.230	-0.225	0.005
0.2341	-0.119	-0.032	-0.205	-0.356	-0.377	-0.021	-0.139	-0.032	-0.205	-0.376	-0.377	-0.001
0.3157	-0.149	-0.040	-0.252	-0.442	-0.458	-0.016	-0.167	-0.040	-0.252	-0.460	-0.458	0.001
0.4200	-0.178	-0.049	-0.292	-0.518	-0.535	-0.017	-0.188	-0.049	-0.292	-0.528	-0.535	-0.007
0.4909	-0.189	-0.052	-0.305	-0.545	-0.548	-0.002	-0.193	-0.052	-0.305	-0.550	-0.548	0.002
0.6059	-0.192	-0.053	-0.300	-0.545	-0.539	0.006	-0.184	-0.053	-0.300	-0.537	-0.539	-0.002
0.6823	-0.182	-0.051	-0.278	-0.510	-0.490	0.020	-0.167	-0.051	-0.278	-0.495	-0.490	0.005
0.7933	-0.146	-0.041	-0.216	-0.404	-0.385	0.019	-0.126	-0.041	-0.216	-0.384	-0.385	-0.001
0.8823	-0.097	-0.028	-0.140	-0.266	-0.248	0.017	-0.080	-0.028	-0.140	-0.248	-0.248	-0.001

<b>303.15 K</b>												
x1	Calculated contribution			V <sup>E</sup>	V <sup>E</sup>	deviation	Calculated contribution with a, b			V <sup>E</sup>	V <sup>E</sup>	deviation
	Interactional	Free volume	P* effect	PFP	exp		Interactional	Free volume	P* effect	PFP	exp	
0.1280	-0.060	-0.023	-0.142	-0.225	-0.237	-0.012	-0.077	-0.023	-0.142	-0.242	-0.237	0.005
0.2341	-0.101	-0.039	-0.235	-0.375	-0.397	-0.022	-0.123	-0.039	-0.235	-0.396	-0.397	-0.001
0.3157	-0.128	-0.049	-0.289	-0.465	-0.483	-0.018	-0.147	-0.049	-0.289	-0.485	-0.483	0.001
0.4200	-0.152	-0.059	-0.334	-0.545	-0.564	-0.019	-0.164	-0.059	-0.334	-0.557	-0.564	-0.007
0.4909	-0.162	-0.063	-0.350	-0.575	-0.577	-0.003	-0.167	-0.063	-0.350	-0.579	-0.577	0.002
0.6059	-0.165	-0.065	-0.345	-0.575	-0.569	0.006	-0.157	-0.065	-0.345	-0.566	-0.569	-0.002
0.6823	-0.157	-0.062	-0.320	-0.538	-0.517	0.021	-0.141	-0.062	-0.320	-0.522	-0.517	0.005
0.7933	-0.127	-0.050	-0.250	-0.427	-0.405	0.021	-0.105	-0.050	-0.250	-0.405	-0.405	-0.001
0.8823	-0.085	-0.034	-0.162	-0.281	-0.262	0.019	-0.065	-0.034	-0.162	-0.261	-0.262	-0.001
<b>313.15 K</b>												
0.1280	-0.049	-0.027	-0.160	-0.237	-0.250	-0.014	-0.069	-0.027	-0.160	-0.256	-0.250	0.006
0.2341	-0.084	-0.046	-0.265	-0.395	-0.419	-0.025	-0.108	-0.046	-0.265	-0.419	-0.419	-0.001
0.3157	-0.106	-0.058	-0.326	-0.490	-0.510	-0.020	-0.127	-0.058	-0.326	-0.512	-0.510	0.001
0.4200	-0.126	-0.070	-0.379	-0.575	-0.595	-0.020	-0.140	-0.070	-0.379	-0.588	-0.595	-0.007
0.4909	-0.135	-0.075	-0.396	-0.606	-0.610	-0.004	-0.140	-0.075	-0.396	-0.612	-0.610	0.002
0.6059	-0.138	-0.077	-0.391	-0.607	-0.600	0.007	-0.129	-0.077	-0.391	-0.598	-0.600	-0.002
0.6823	-0.131	-0.074	-0.363	-0.569	-0.546	0.022	-0.114	-0.074	-0.363	-0.551	-0.546	0.005
0.7933	-0.107	-0.061	-0.284	-0.451	-0.427	0.024	-0.082	-0.061	-0.284	-0.427	-0.427	0.000
0.8823	-0.072	-0.041	-0.185	-0.297	-0.276	0.021	-0.050	-0.041	-0.185	-0.276	-0.276	-0.001

<b>323.15 K</b>												
x1	Calculated contribution			V <sup>E</sup>	V <sup>E</sup>	deviation	Calculated contribution with a, b			V <sup>E</sup>	V <sup>E</sup>	deviation
	Interactional	Free volume	P* effect	PFP	exp		Interactional	Free volume	P* effect	PFP	exp	
0.1280	-0.040	-0.031	-0.179	-0.249	-0.265	-0.015	-0.061	-0.031	-0.179	-0.271	-0.265	0.006
0.2341	-0.067	-0.053	-0.296	-0.416	-0.443	-0.027	-0.094	-0.053	-0.296	-0.443	-0.443	0.000
0.3157	-0.085	-0.067	-0.365	-0.517	-0.540	-0.023	-0.109	-0.067	-0.365	-0.541	-0.540	0.002
0.4200	-0.102	-0.081	-0.424	-0.607	-0.629	-0.022	-0.117	-0.081	-0.424	-0.622	-0.629	-0.007
0.4909	-0.109	-0.088	-0.444	-0.640	-0.645	-0.005	-0.115	-0.088	-0.444	-0.647	-0.645	0.002
0.6059	-0.112	-0.091	-0.439	-0.642	-0.635	0.007	-0.102	-0.091	-0.439	-0.632	-0.635	-0.003
0.6823	-0.107	-0.087	-0.408	-0.602	-0.577	0.024	-0.087	-0.087	-0.408	-0.582	-0.577	0.005
0.7933	-0.087	-0.071	-0.320	-0.478	-0.451	0.027	-0.060	-0.071	-0.320	-0.451	-0.451	0.000
0.8823	-0.058	-0.048	-0.209	-0.315	-0.291	0.024	-0.034	-0.048	-0.209	-0.291	-0.291	-0.001
<b>333.15 K</b>												
0.1280	-0.031	-0.035	-0.198	-0.264	-0.281	-0.018	-0.055	-0.035	-0.198	-0.287	-0.281	0.006
0.2341	-0.053	-0.060	-0.327	-0.440	-0.470	-0.030	-0.082	-0.060	-0.327	-0.470	-0.470	0.000
0.3157	-0.066	-0.077	-0.404	-0.547	-0.573	-0.026	-0.094	-0.077	-0.404	-0.574	-0.573	0.002
0.4200	-0.080	-0.093	-0.469	-0.642	-0.667	-0.025	-0.097	-0.093	-0.469	-0.660	-0.667	-0.008
0.4909	-0.086	-0.100	-0.492	-0.678	-0.684	-0.006	-0.093	-0.100	-0.492	-0.686	-0.684	0.002
0.6059	-0.088	-0.104	-0.487	-0.680	-0.672	0.007	-0.077	-0.104	-0.487	-0.669	-0.672	-0.003
0.6823	-0.084	-0.100	-0.454	-0.638	-0.611	0.027	-0.063	-0.100	-0.454	-0.617	-0.611	0.005
0.7933	-0.069	-0.082	-0.356	-0.507	-0.477	0.031	-0.038	-0.082	-0.356	-0.477	-0.477	0.000
0.8823	-0.046	-0.056	-0.233	-0.335	-0.308	0.027	-0.019	-0.056	-0.233	-0.307	-0.308	0.000

**343.15 K**

x1	Calculated contribution			V <sup>E</sup>	V <sup>E</sup>	deviation	Calculated contribution with a, b			V <sup>E</sup>	V <sup>E</sup>	deviation
	Interactional	Free volume	P* effect	PFP	exp		Interactional	Free volume	P* effect	PFP	exp	
0.1280	-0.023	-0.039	-0.216	-0.279	-0.299	-0.020	-0.050	-0.039	-0.216	-0.306	-0.299	0.007
0.2341	-0.040	-0.068	-0.358	-0.466	-0.499	-0.033	-0.073	-0.068	-0.358	-0.499	-0.499	0.000
0.3157	-0.050	-0.087	-0.443	-0.579	-0.609	-0.029	-0.081	-0.087	-0.443	-0.610	-0.609	0.002
0.4200	-0.060	-0.105	-0.515	-0.681	-0.708	-0.027	-0.080	-0.105	-0.515	-0.701	-0.708	-0.008
0.4909	-0.065	-0.114	-0.541	-0.719	-0.726	-0.007	-0.073	-0.114	-0.541	-0.728	-0.726	0.002
0.6059	-0.067	-0.118	-0.536	-0.722	-0.714	0.008	-0.055	-0.118	-0.536	-0.710	-0.714	-0.004
0.6823	-0.064	-0.114	-0.499	-0.678	-0.649	0.029	-0.040	-0.114	-0.499	-0.654	-0.649	0.005
0.7933	-0.053	-0.094	-0.393	-0.539	-0.504	0.035	-0.018	-0.094	-0.393	-0.505	-0.504	0.001
0.8823	-0.036	-0.064	-0.257	-0.356	-0.325	0.031	-0.004	-0.064	-0.257	-0.325	-0.325	0.000

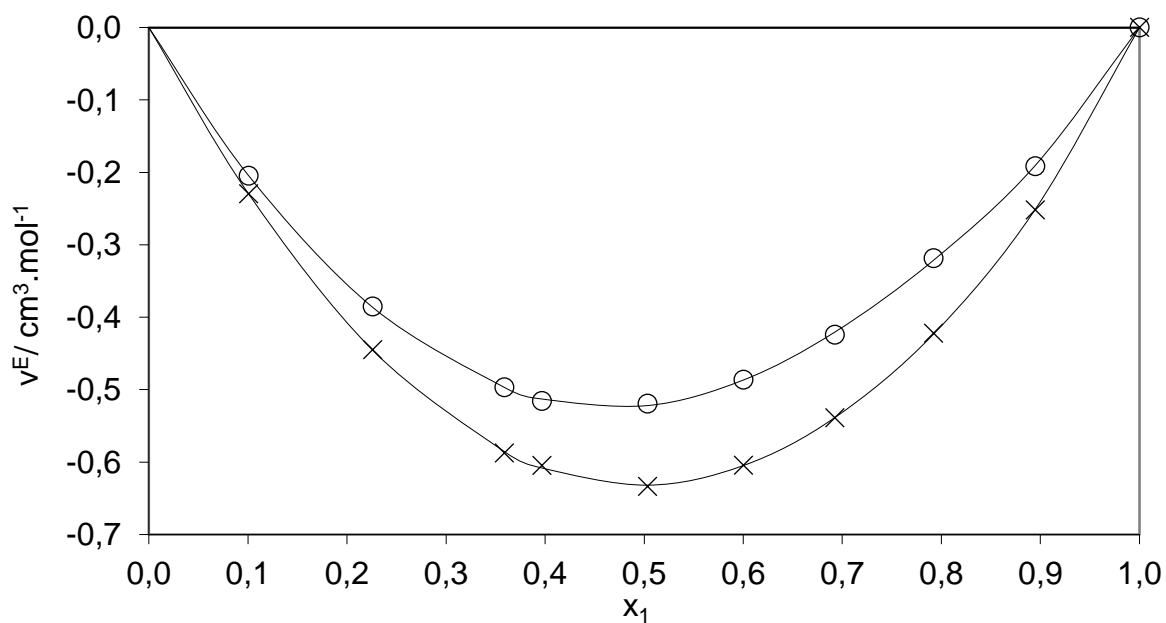


Figure 1: Excess molar volume ( $v^E$ ) for the furan(1) + MDEA(2) binary system as a function of mole fraction  $x_1$  at atmospheric pressure  $p$  and two different temperatures  $T$ : (unfilled circle) 278.15 K; (cross) 303.15 K; solid line, Redlich–Kister correlation.

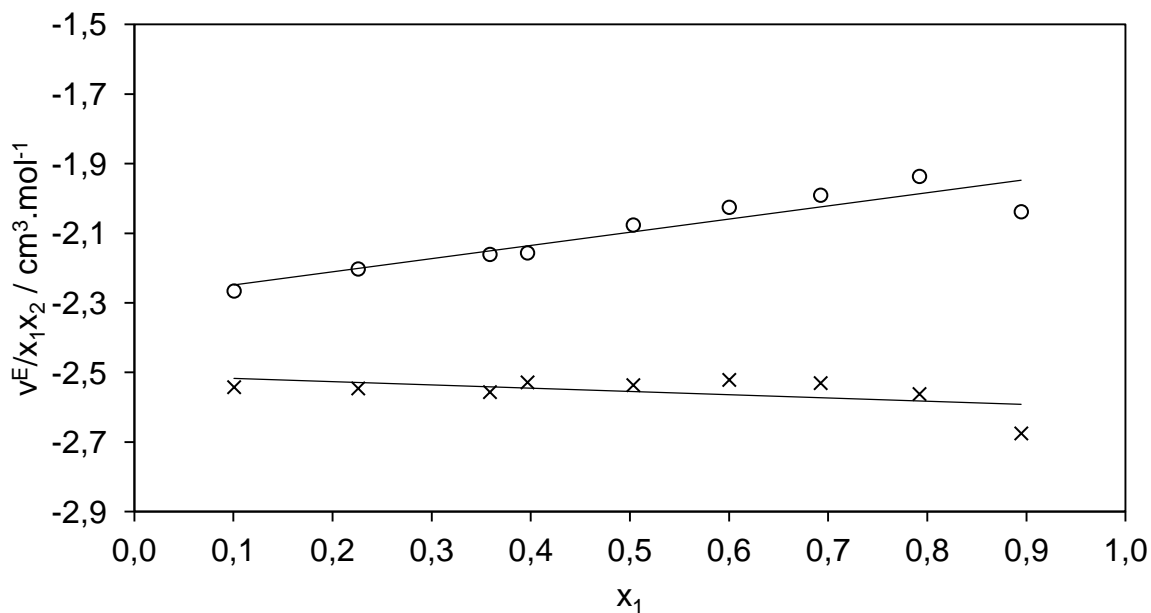


Figure 2: Plot of  $v^E/x_1x_2$  for the furan(1) + MDEA(2) system as a function of the furan mole fraction  $x_1$  at atmospheric pressure  $p$  and two different temperatures  $T$ : (unfilled circle) 278.15 K; (cross) 303.15 K; solid line, Redlich–Kister correlation.

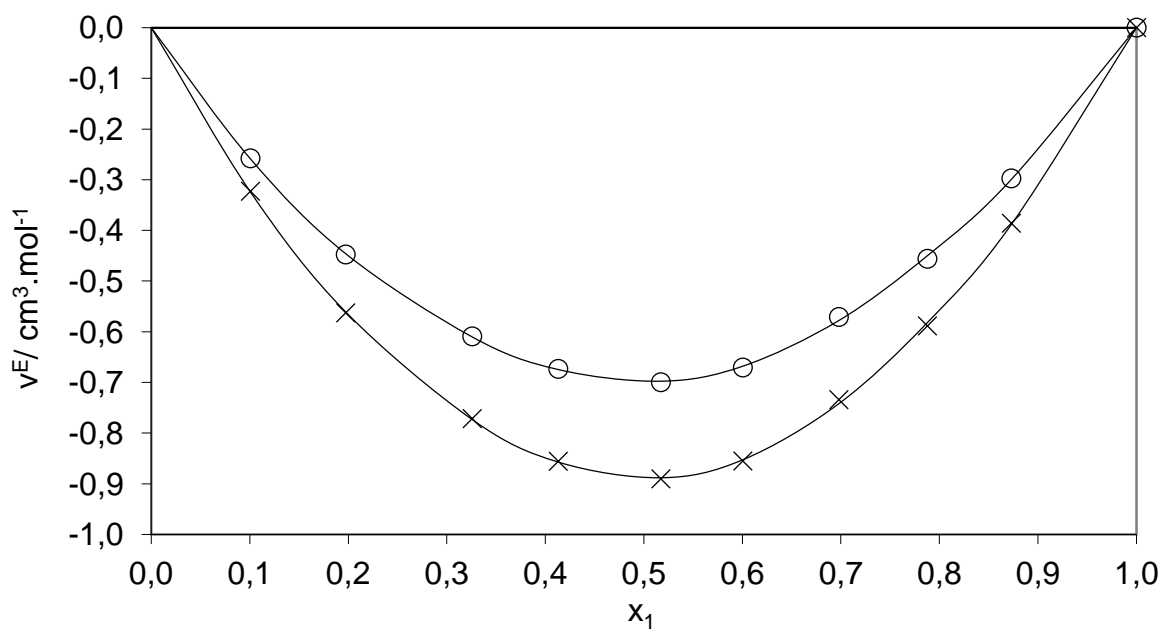


Figure 3: Excess molar volume ( $v^E$ ) for the furan(1) + DEG(2) binary system as a function of mole fraction  $x_1$  at atmospheric pressure  $p$  and two different temperatures  $T$ : (unfilled circle) 278.15 K; (cross) 303.15 K; solid line, Redlich–Kister correlation.

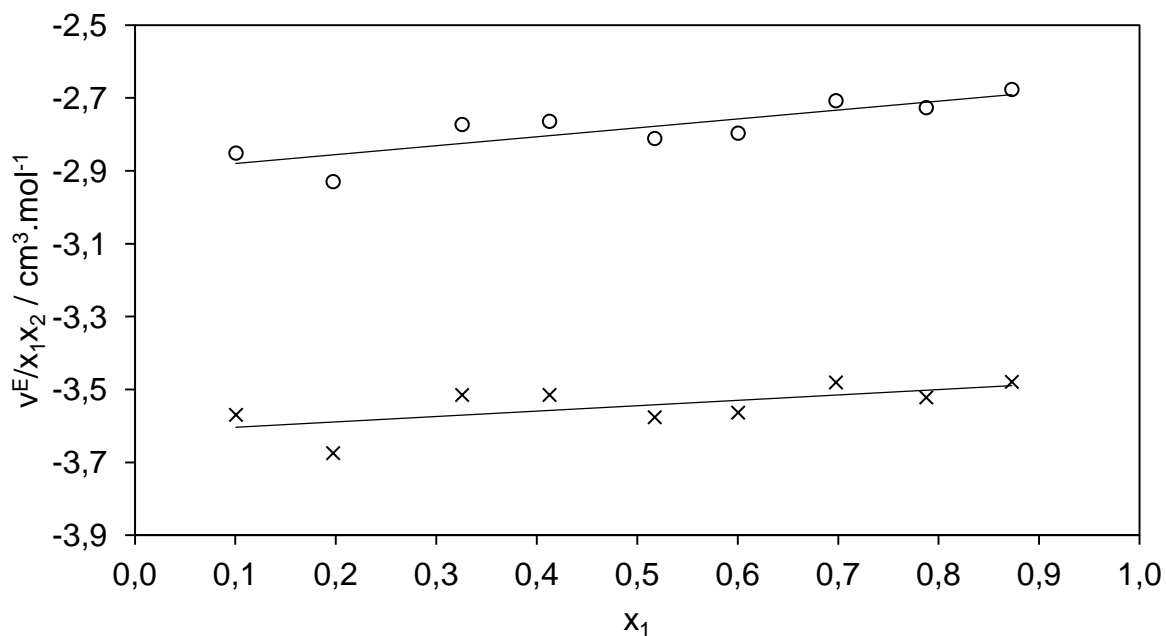


Figure 4: Plot of  $v^E/x_1x_2$  for the furan(1) + DEG(2) system as a function of the furan mole fraction  $x_1$  at atmospheric pressure  $p$  and two different temperatures  $T$ : (unfilled circle) 278.15 K; (cross) 303.15 K; solid line, Redlich–Kister correlation.

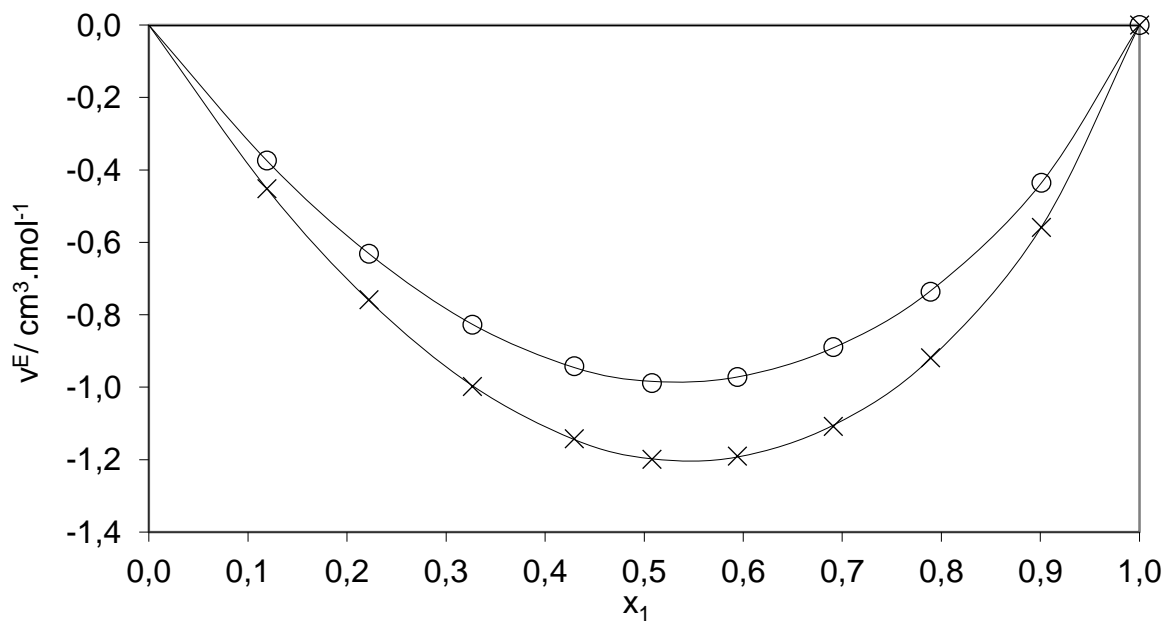


Figure 5: Excess molar volume ( $v^E$ ) for the furan(1) + TEG(2) binary system as a function of mole fraction  $x_1$  at atmospheric pressure  $p$  and two different temperatures  $T$ : (unfilled circle) 278.15 K; (cross) 303.15 K; solid line, Redlich–Kister correlation.

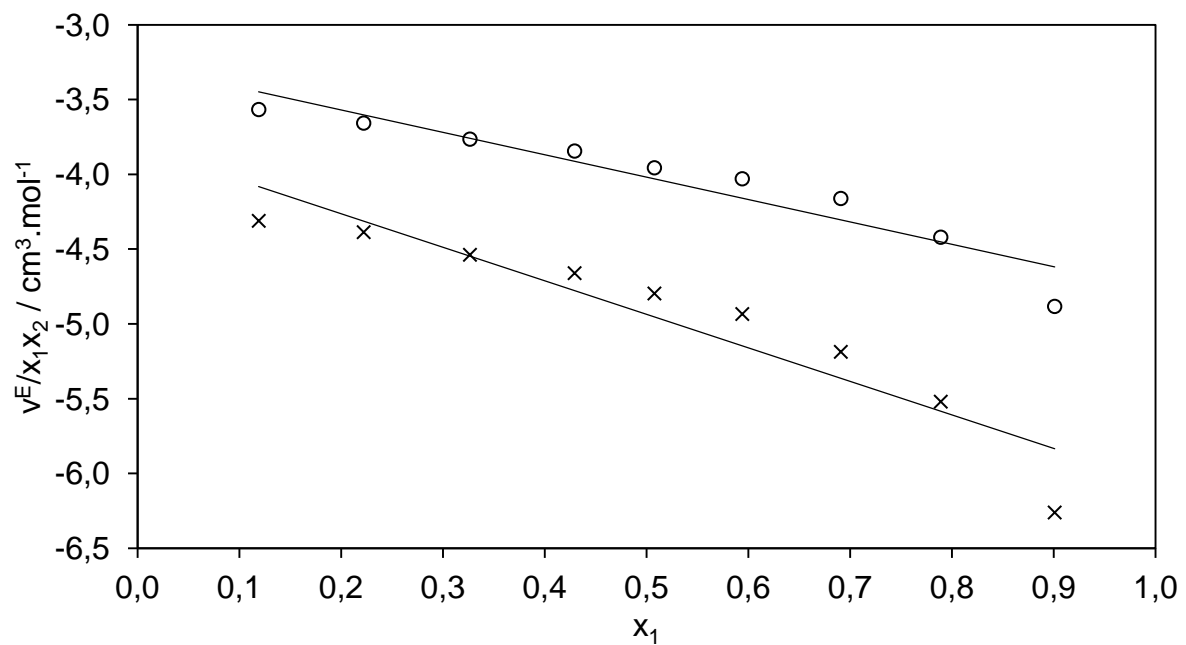


Figure 6: Plot of  $v^E/x_1x_2$  for the furan(1) + TEG(2) system as a function of the furan mole fraction  $x_1$  at atmospheric pressure  $p$  and two different temperatures  $T$ : (unfilled circle) 278.15 K; (cross) 303.15 K; solid line, Redlich–Kister correlation.

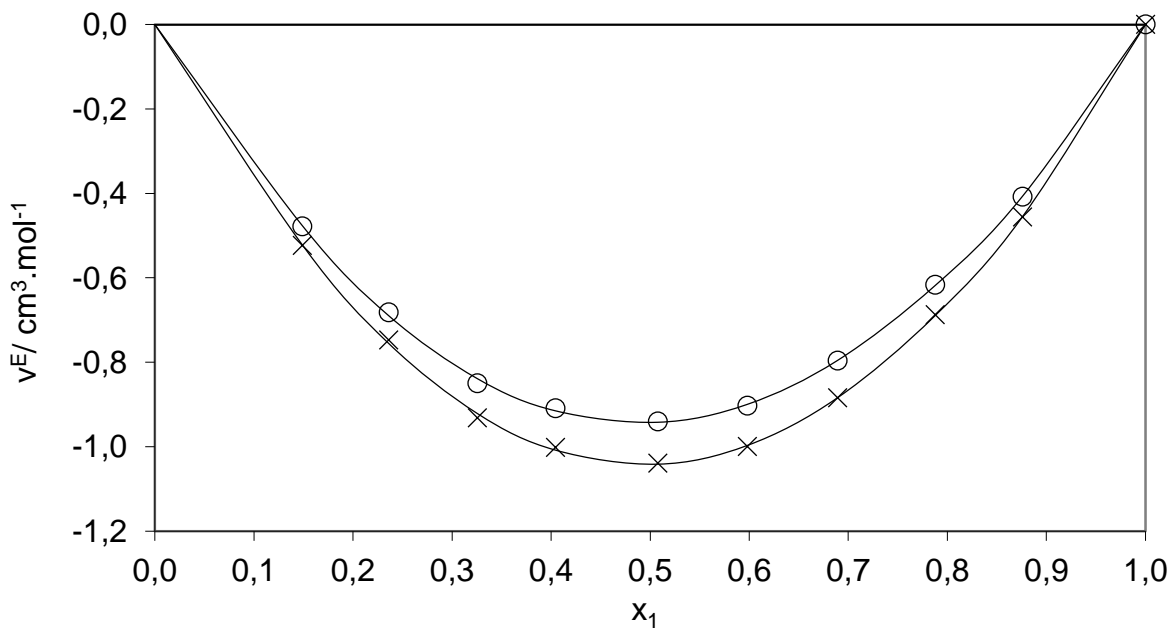


Figure 7: Excess molar volume ( $v^E$ ) for the furan(1) + DMA(2) binary system as a function of mole fraction  $x_1$  at atmospheric pressure  $p$  and two different temperatures  $T$ : (unfilled circle) 278.15 K; (cross) 303.15 K; solid line, Redlich–Kister correlation.

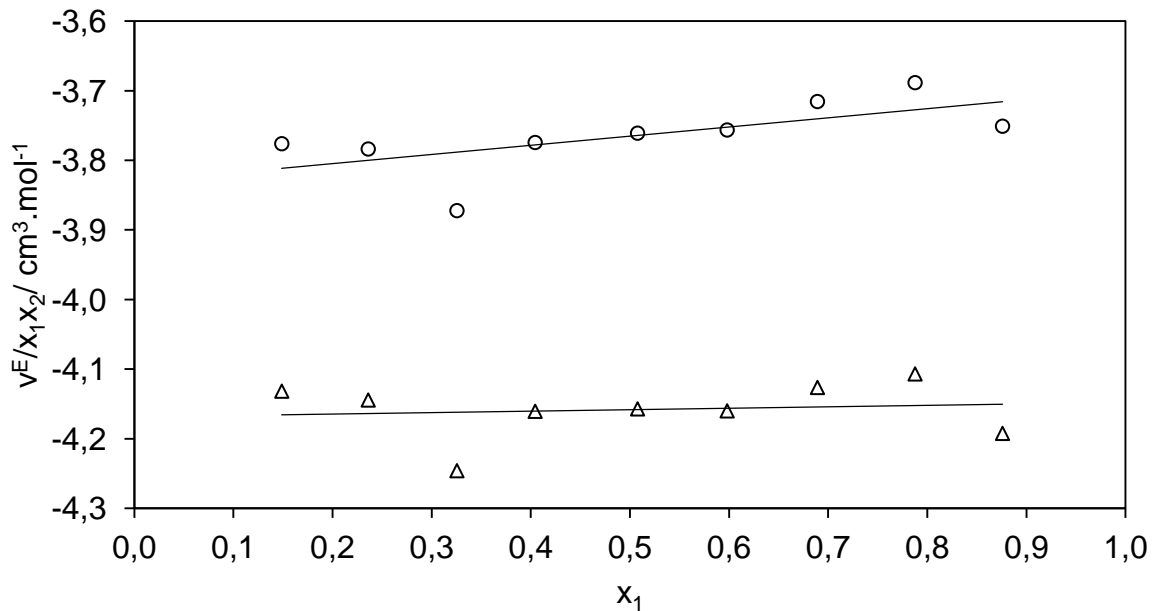


Figure 8: Plot of  $v^E/x_1x_2$  for the furan(1) + DMA(2) system as a function of the furan mole fraction  $x_1$  at atmospheric pressure  $p$  and two different temperatures  $T$ : (unfilled circle) 278.15 K; (cross) 303.15 K; solid line, Redlich–Kister correlation.



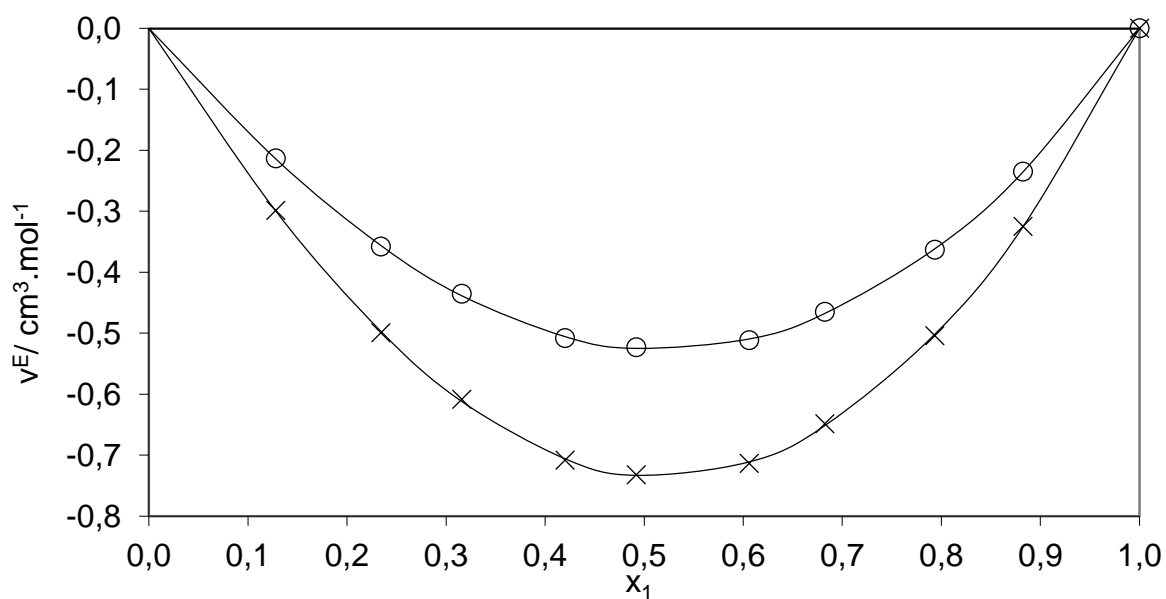


Figure 9: Excess molar volume ( $v^E$ ) for the DMF(1) + DMA(2) binary system as a function of mole fraction  $x_1$  at atmospheric pressure  $p$  and two different temperatures  $T$ : (unfilled circle) 283.15 K; (cross) 343.15 K; solid line, Redlich–Kister correlation

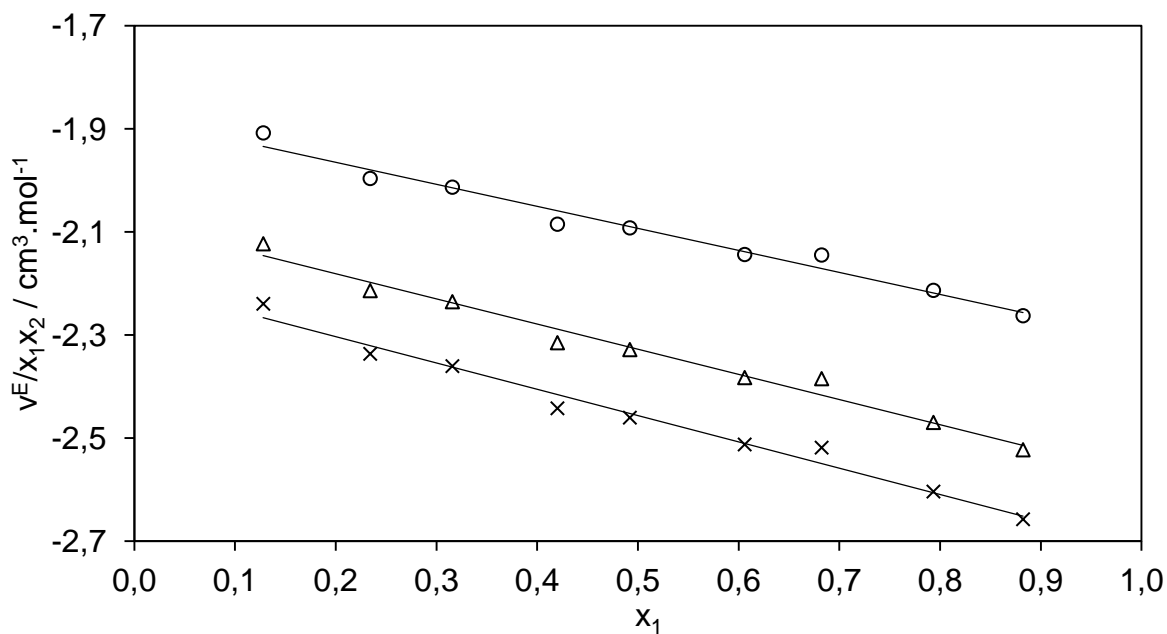


Figure 10: Plot of  $v^E/x_1x_2$  for the DMF(1) + DMA(2) system as a function of the furan mole fraction  $x_1$  at atmospheric pressure  $p$  and two different temperatures  $T$ : (unfilled circle) 283.15 K; (triangle) 313.15 K; (cross) 303.15 K; solid line, Redlich–Kister correlation.

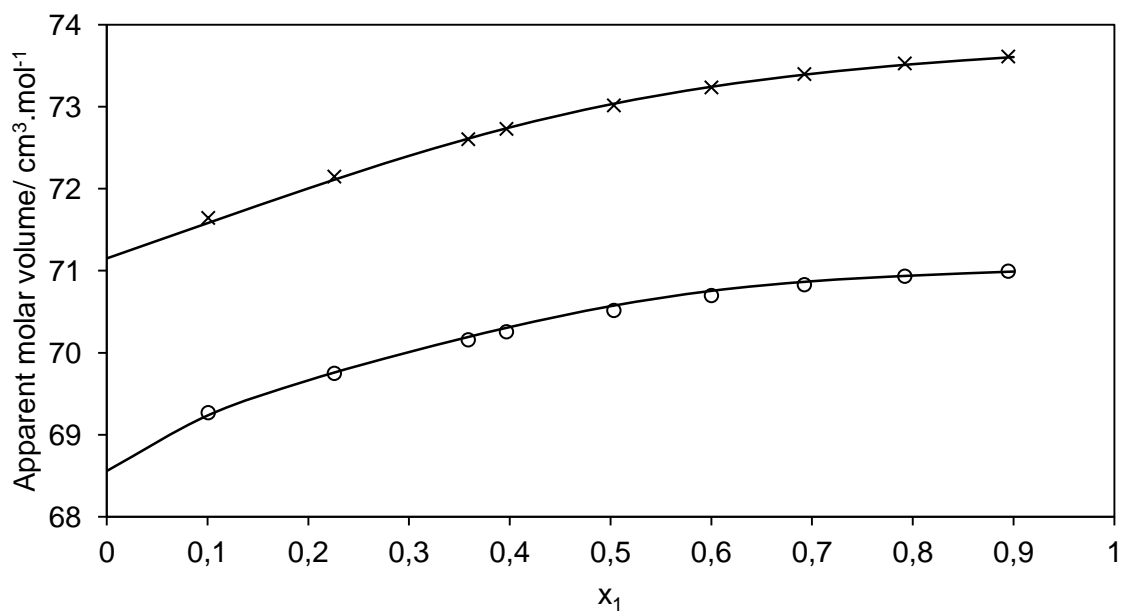


Figure 11: Calculated apparent molar volume using the Redlich–Kister correlation (solid line) and experimental apparent molar volume (symbols) of the furan(1) + MDEA(2) system as a function of the furan mole fraction  $x_1$  at atmospheric pressure  $p$  and two different temperatures  $T$ : (unfilled circle) 278.15 K, (cross) 303.15 K.

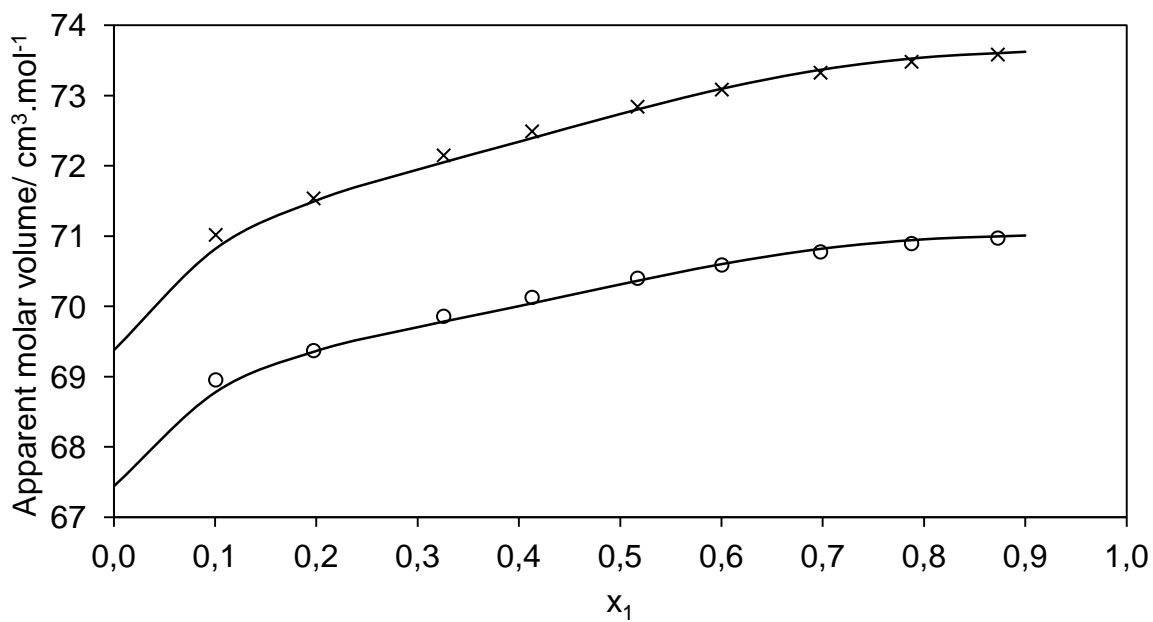


Figure 12: Calculated apparent molar volume using the Redlich–Kister correlation (solid line) and experimental apparent molar volume (symbols) of the furan(1) + DEG(2) system as a function of the furan mole fraction  $x_1$  at atmospheric pressure  $p$  and two different temperatures  $T$ : (unfilled circle) 278.15 K, (cross) 303.15 K.

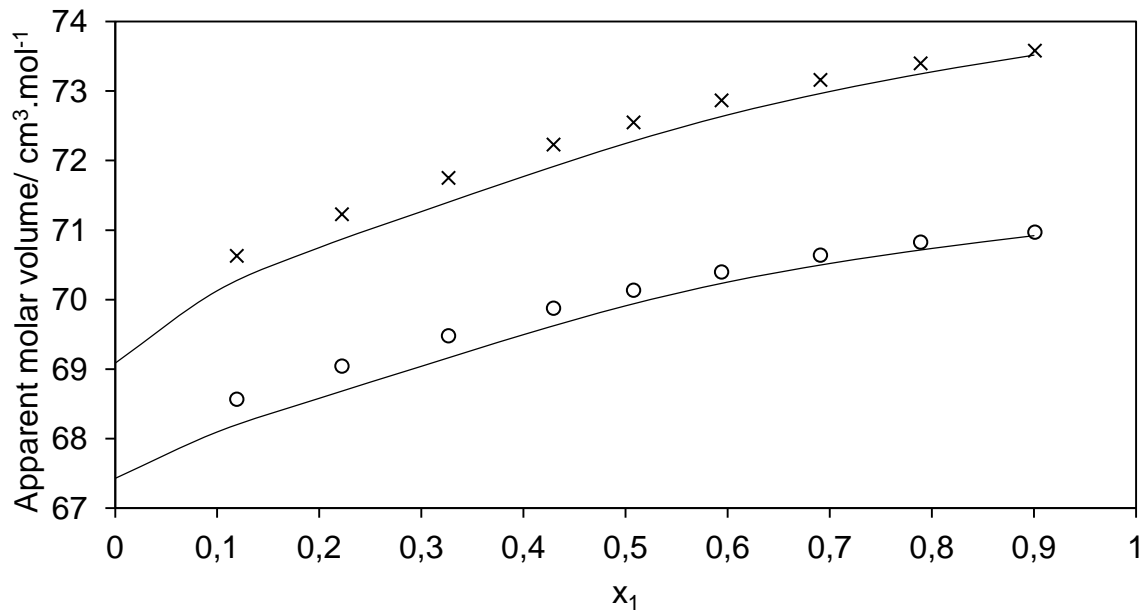


Figure 13: Calculated apparent molar volume using the Redlich–Kister correlation (solid line) and experimental apparent molar volume (symbols) of the furan(1) + TEG(2) system as a function of the furan mole fraction  $x_1$  at atmospheric pressure  $p$  and two different temperatures  $T$ : (unfilled circle) 278.15 K, (cross) 303.15 K.

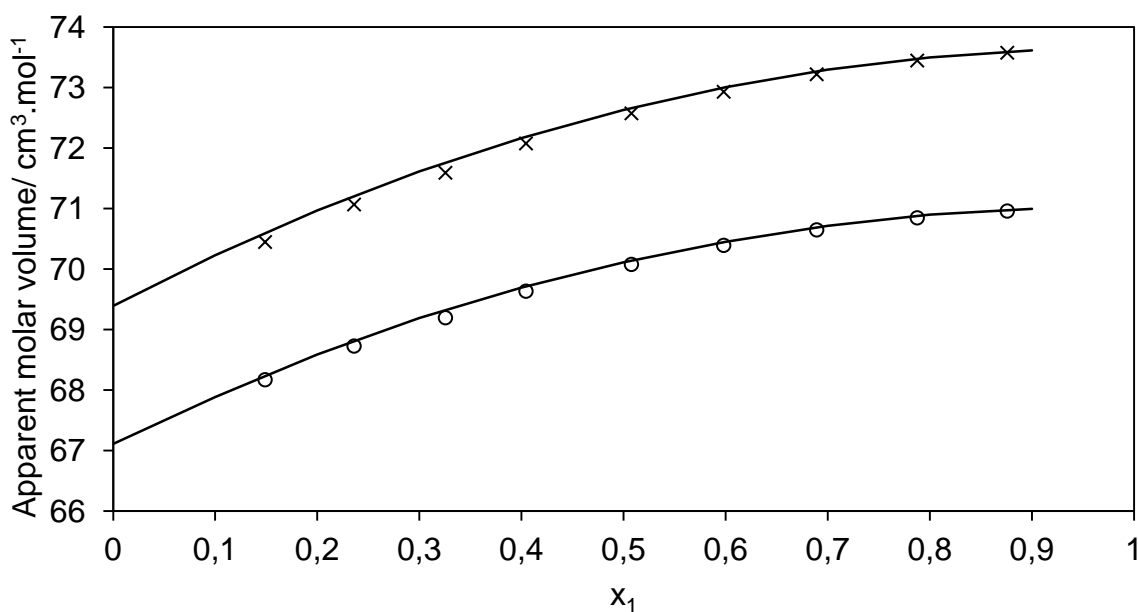


Figure 14: Calculated apparent molar volume using the Redlich–Kister correlation (solid line) and experimental apparent molar volume (symbols) of the furan(1) + DMA(2) system as a function of the furan mole fraction  $x_1$  at atmospheric pressure  $p$  and two different temperatures  $T$ : (unfilled circle) 278.15 K, (cross) 303.15 K.

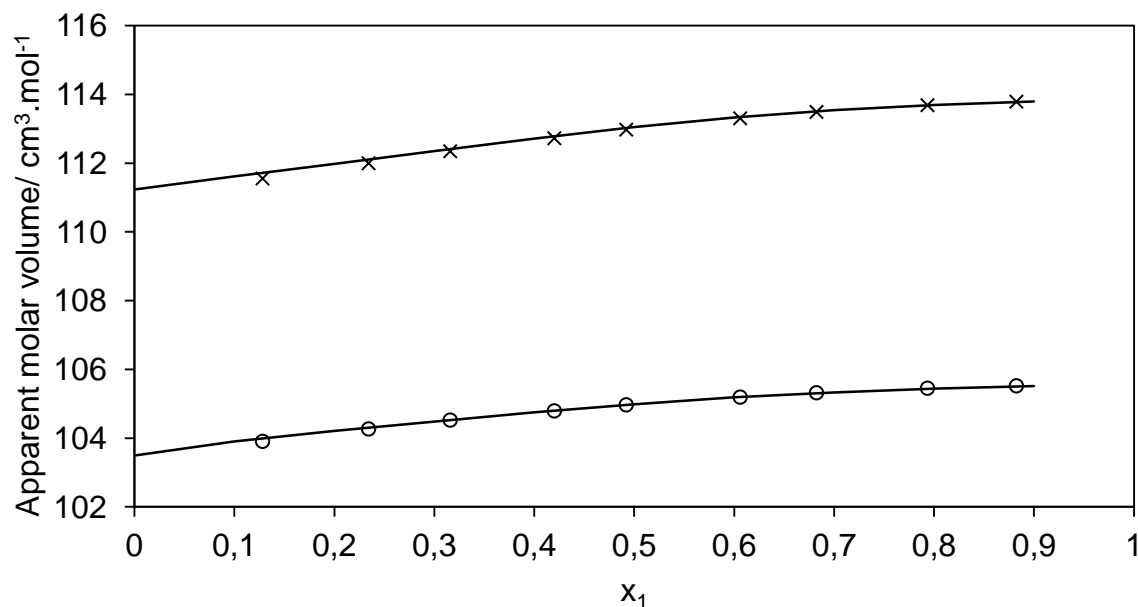
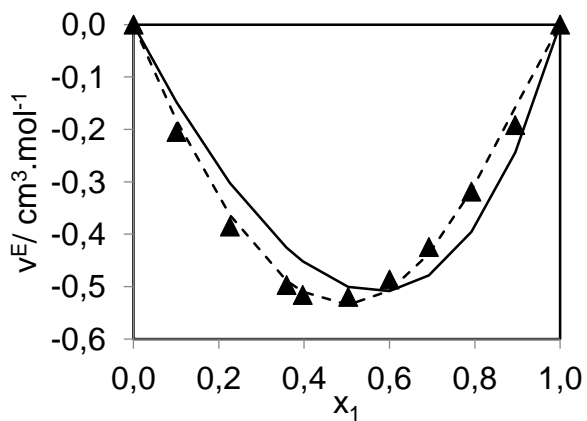
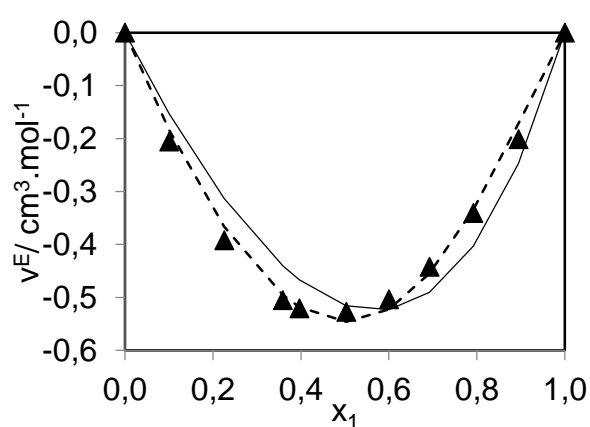


Figure 15: Calculated apparent molar volume using the Redlich–Kister correlation (solid line) and experimental apparent molar volume (symbols) of the DMF(1) + DMA(2) system as a function of the

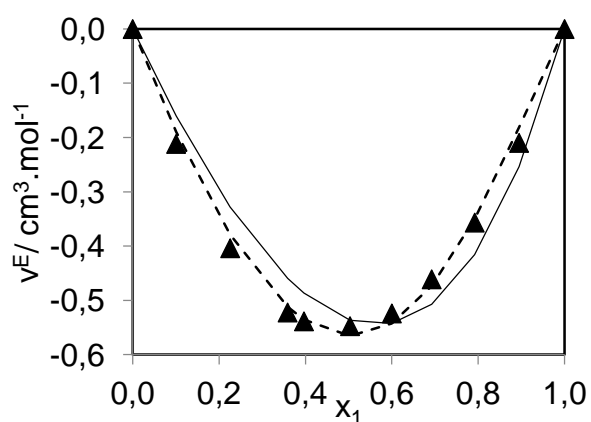
furan mole fraction  $x_1$  at atmospheric pressure  $p$  and two different temperatures  $T$ : (unfilled circle) 283.15 K, (cross) 343.15 K.



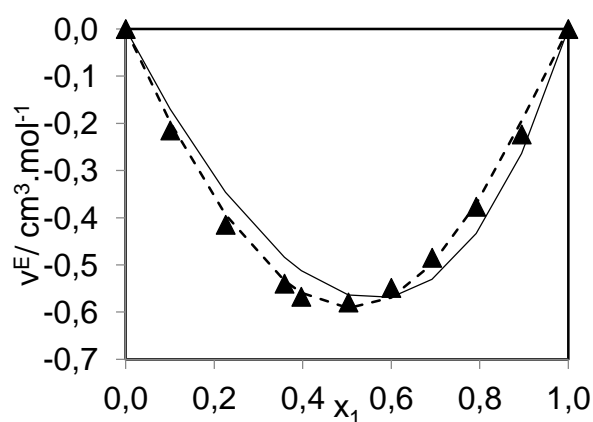
a)



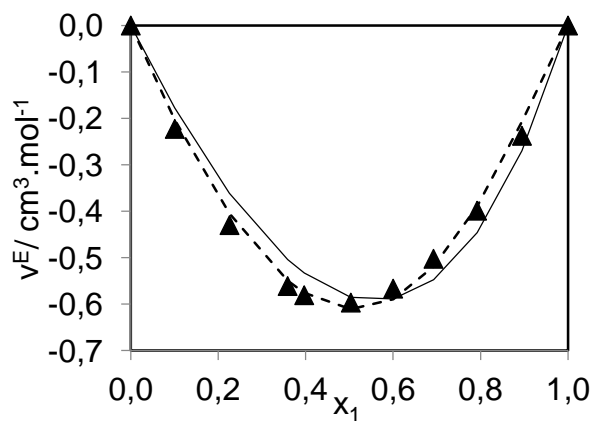
b)



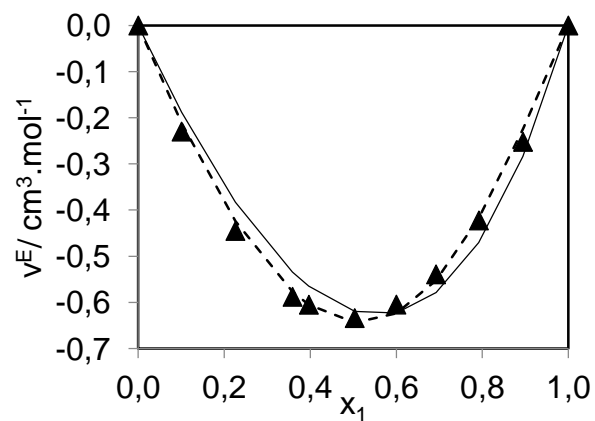
c)



d)

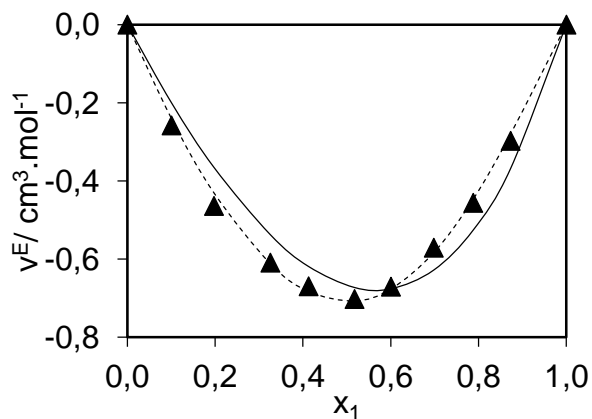


e)

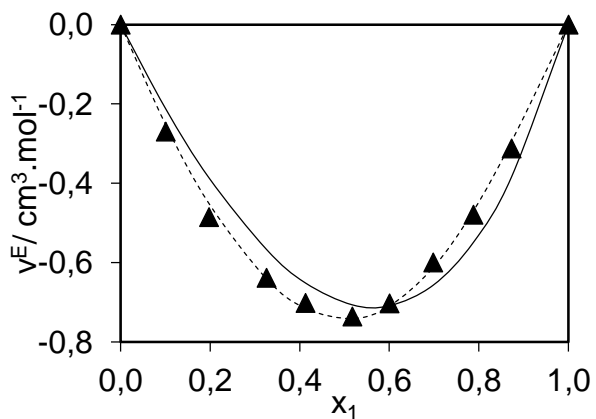


f)

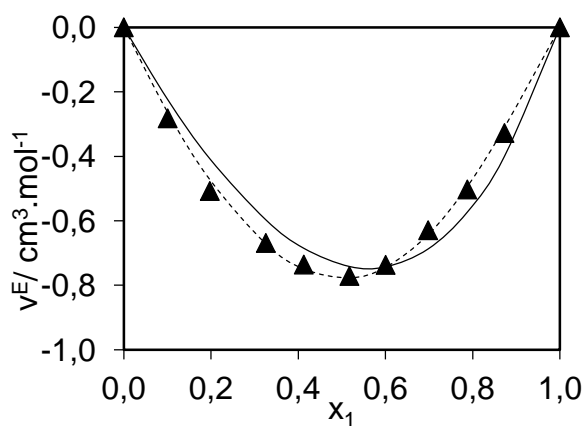
Figure 16: Excess volumes for the furan(1) + MDEA(2) binary system at  $T/ K=278.15$  (a),  $283.15$  (b),  $288.15$  (c),  $293.15$  (d),  $298.15$  (e), and  $303.15$  (f) as a function of the mole fraction  $x_1$ . Symbols, experimental data; solid line, calculated using the PFP model with constant value of  $X_{12}$ ; dashed line, calculated with the PFP model with  $X_{12}$  being composition dependent.



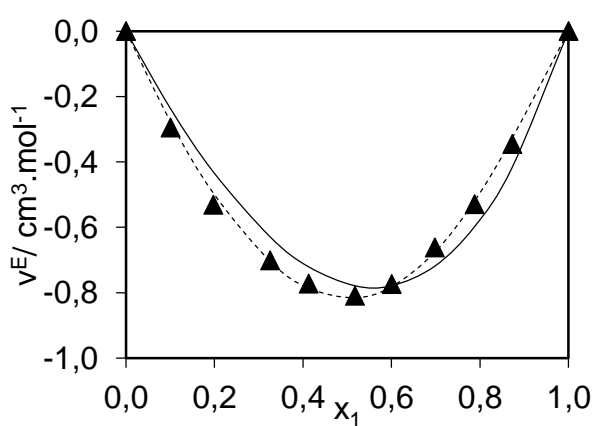
a)



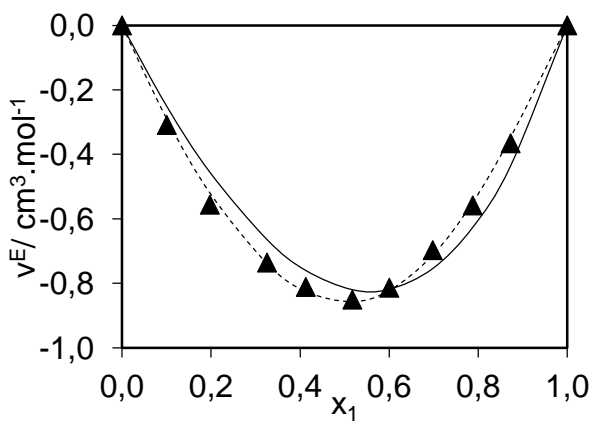
b)



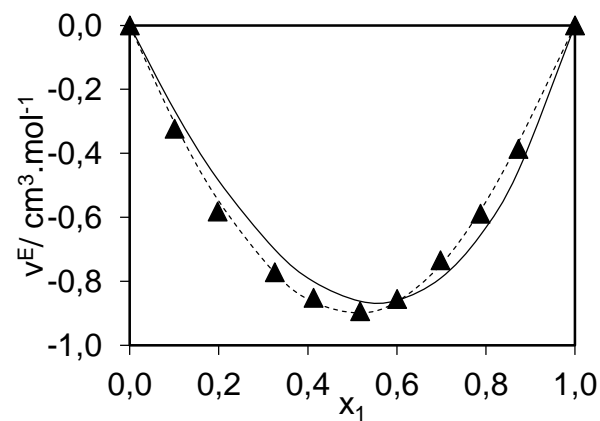
c)



d)

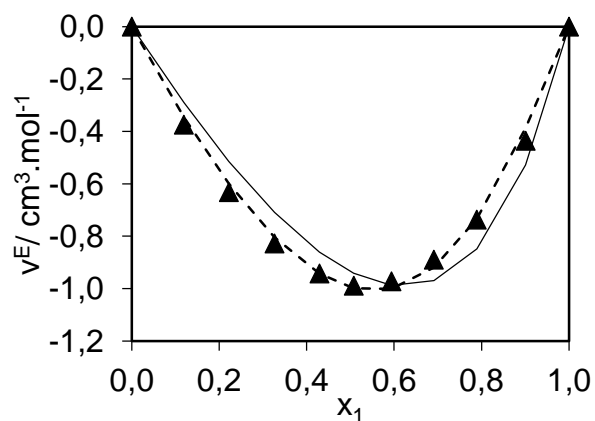


e)

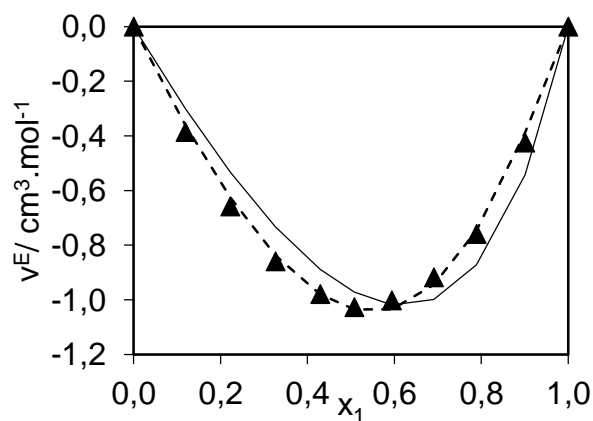


f)

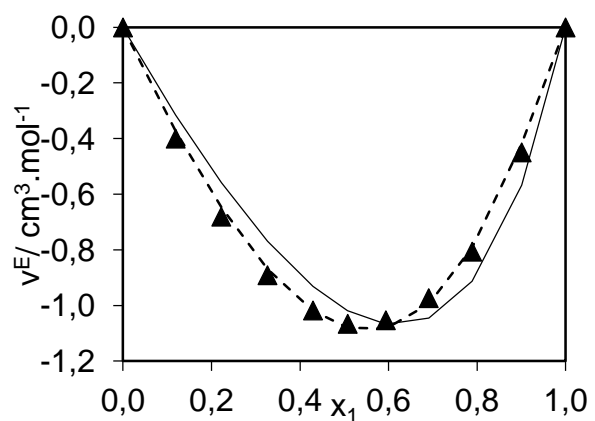
Figure 17: Excess volumes for the furan(1) + DEG(2) binary system at  $T/ K=278.15$  (a),  $283.15$  (b),  $288.15$  (c),  $293.15$  (d),  $298.15$  (e), and  $303.15$  (f) as a function of the mole fraction  $x_1$ . Symbols, experimental data; solid line, calculated using the PFP model with constant value of  $X_{12}$ ; dashed line, calculated with the PFP model with  $X_{12}$  being composition dependent.



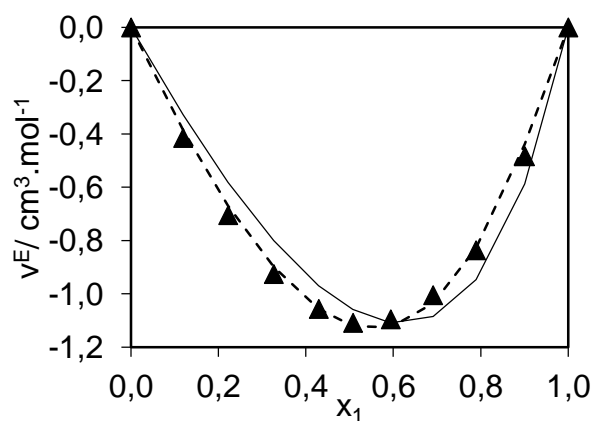
a)



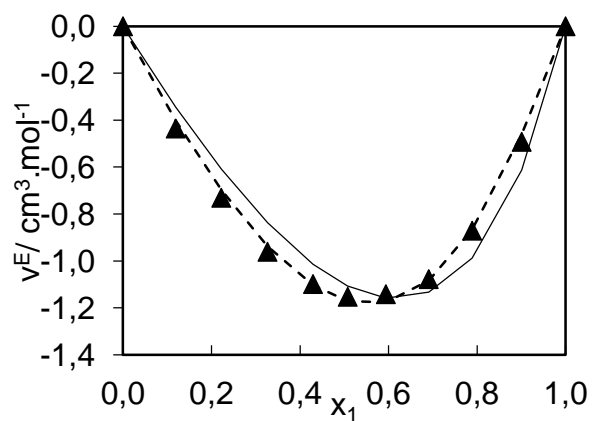
b)



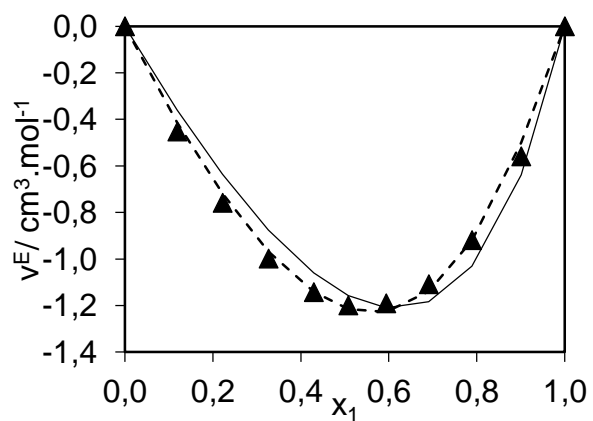
c)



d)



e)



f)

Figure 18: Excess volumes for the furan(1) + TEG(2) binary system at  $T/ K=278.15$  (a),  $283.15$  (b),  $288.15$  (c),  $293.15$  (d),  $298.15$  (e), and  $303.15$  (f) as a function of the mole fraction  $x_1$ . Symbols, experimental data; solid line, calculated using the PFP model with constant value of  $X_{12}$ ; dashed line, calculated with the PFP model with  $X_{12}$  being composition dependent.



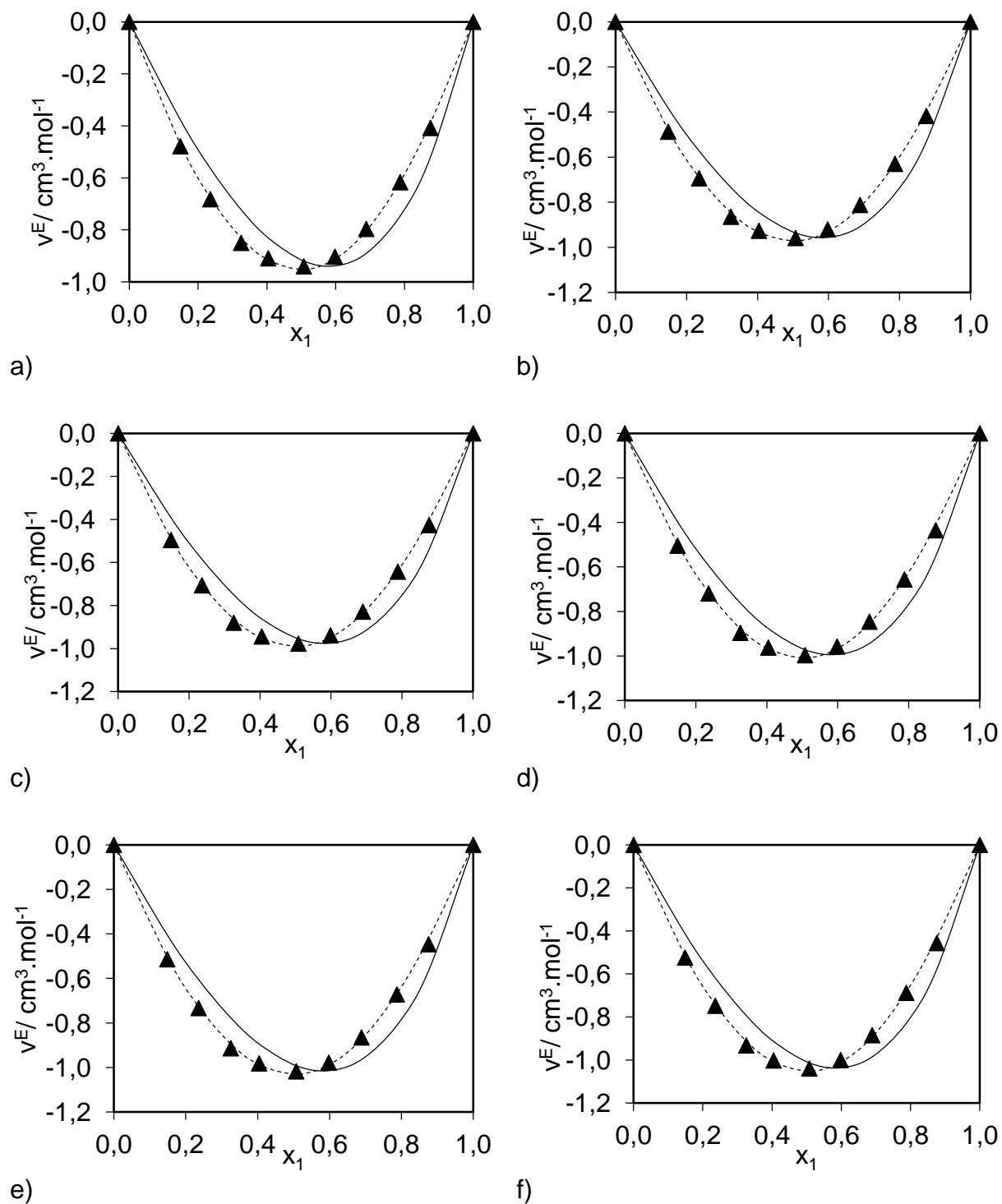
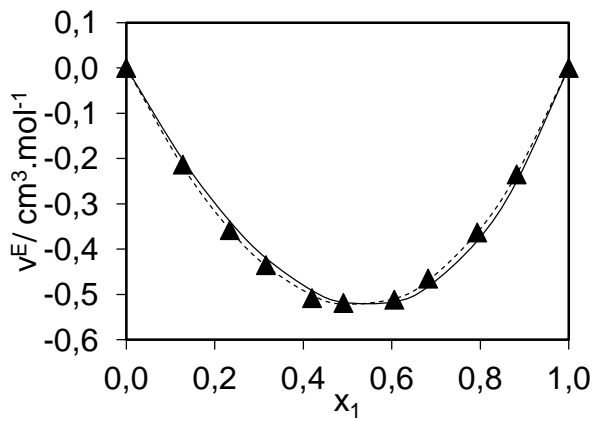
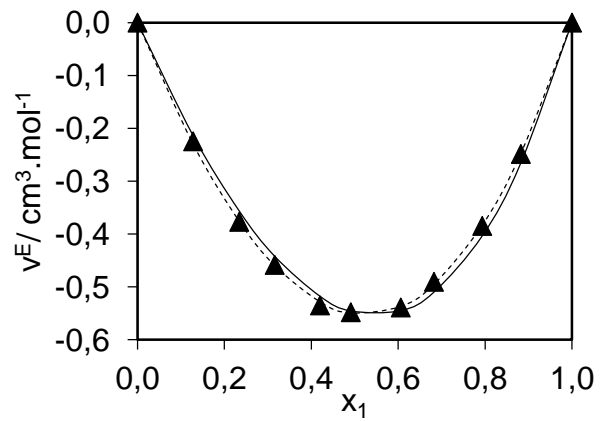


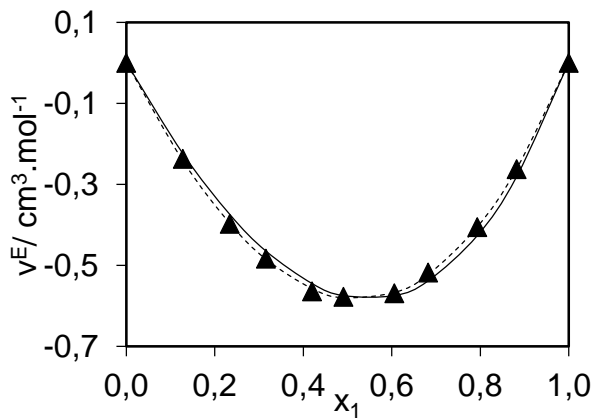
Figure 19: Excess volumes for the furan(1) + DMA(2) binary system at  $T/ \text{K} = 278.15$  (a),  $283.15$  (b),  $288.15$  (c),  $293.15$  (d),  $298.15$  (e), and  $303.15$  (f) as a function of the mole fraction  $x_1$ . Symbols, experimental data; solid line, calculated using the PFP model with constant value of  $X_{12}$ ; dashed line, calculated with the PFP model with  $X_{12}$  being composition dependent.



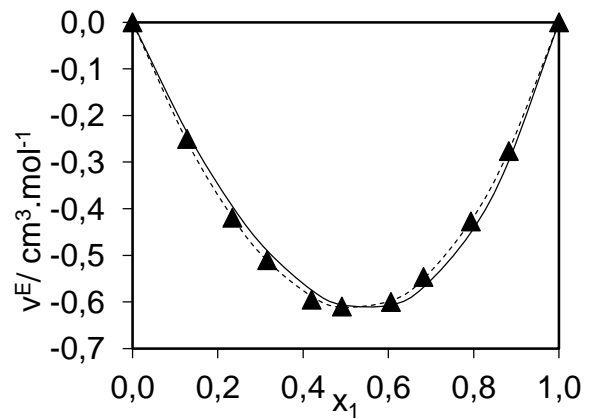
a)



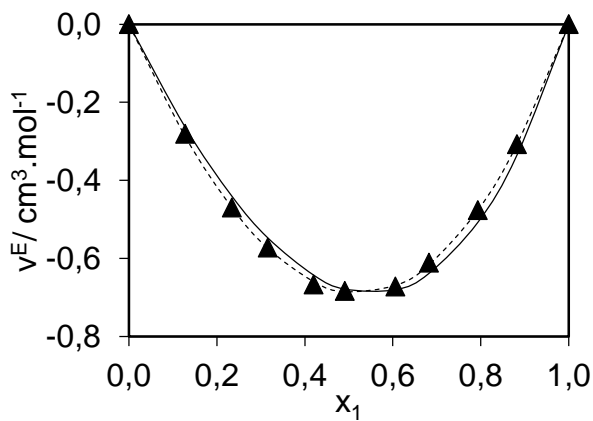
b)



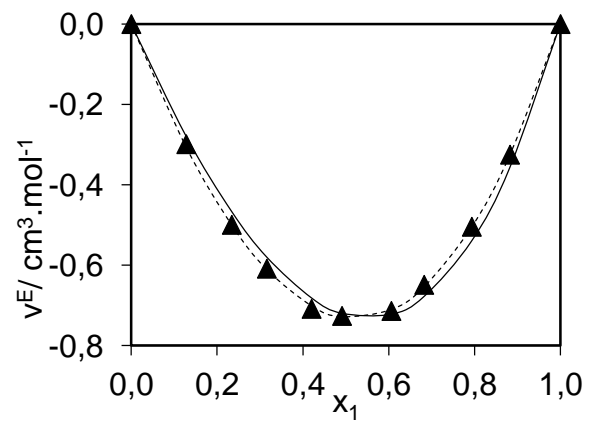
c)



d)



e)



f)

Figure 20: Excess volumes for the DMF(1) + DMA(2) binary system at  $T/ K=283.15$  (a),  $293.15$  (b),  $303.15$  (c),  $323.15$  (d),  $333.15$  (e), and  $343.15$  (f) as a function of the mole fraction  $x_1$ . Symbols, experimental data; solid line, calculated using the PFP model with constant value of  $X_{12}$ ; dashed line, calculated with the PFP model with  $X_{12}$  being composition dependent.

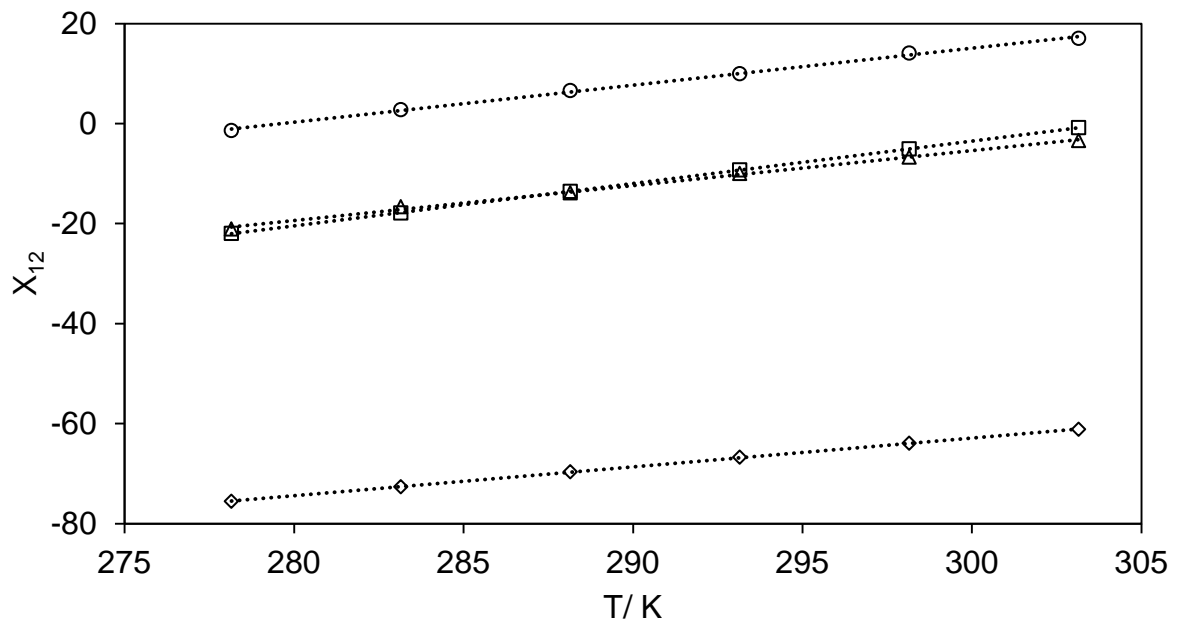


Figure 21: Evolution of the  $X_{12}$  parameters as a function of temperature: (circle), furan + MDEA binary system; (triangle), furan + TEG binary system; (square), furan + DEG binary system; (diamond), furan + DMA binary system

# For Table of Contents Only

